Geochemical Journal, Vol. 50, pp. 3 to 25, 2016 doi:10.2343/geochemj.2.0377

INVITED REVIEW

Presolar silicate grains: Abundances, isotopic and elemental compositions, and the effects of secondary processing

CHRISTINE FLOSS[1,2]* and PIERRE HAENECOUR[1,3]

[1]Laboratory for Space Sciences, Washington University, One Brookings Drive, St. Louis, MO 63130, U.S.A.
[2]Physics Department, Washington University, One Brookings Drive, St. Louis, MO 63130, U.S.A.
[3]Department of Earth and Planetary Sciences, Washington University, One Brookings Drive, St. Louis, MO 63130, U.S.A.

(*Received November 11, 2014; Accepted June 7, 2015*)

Close to a thousand presolar silicate grains have been identified since their initial discovery in interplanetary dust particles (IDPs) just over ten years ago. Studies have shown that silicates are the most abundant type of presolar grain other than nanodiamonds, with abundances of ~200 ppm in the most primitive meteorites and upwards of ~400 ppm in anhydrous IDPs. The oxygen isotopic compositions of presolar silicates are similar to those of presolar oxides, with the majority of the grains originating in low-mass red giant or asymptotic giant branch stars of close-to-solar metallicity. The vast majority of the grains are ferromagnesian silicates with high Fe concentrations. This, together with TEM studies indicating that many presolar silicates have amorphous structures with heterogeneous and non-stoichiometric compositions, suggests that conditions in the stellar environments in which these grains formed were variable and rapidly changing, with grain condensation under non-equilibrium kinetic conditions. Presolar silicates also reflect secondary processes taking place in the solar nebula and the parent bodies of the meteorites in which they are found. Abundance variations within individual meteorites provide constraints on secondary processes, and both thermal metamorphism and aqueous alteration result in changes to the elemental compositions of the grains. Studies of presolar silicates complement those of other presolar grain types, providing additional constraints on stellar environments and nucleosynthetic processes.

Keywords: presolar grains, silicates, nucleosynthesis, isotopes, AGB stars

INTRODUCTION AND HISTORICAL BACKGROUND

Presolar grains are stellar condensates that form in the outflows of evolved stars and in the ejecta of stellar explosions (novae and supernovae). They survived the formation of the solar system and are recognized by their isotopic signatures, which differ substantially (e.g., order of magnitude variations) from those observed in other solar system materials (Zinner, 2014). First identified in the mid-1980s, these grains can be studied in the laboratory to gain a better understanding of nucleosynthesis of the elements and stellar and galactic chemical evolution. They also provide information about conditions in the stellar sources in which they formed and the environments they have traversed subsequent to formation, including the interstellar medium (ISM), the early solar nebula and the parent bodies of the meteorites in which they are found.

Evidence for the possible survival of presolar grains initially came from the observation of isotopic anomalies in hydrogen (Boato, 1954), neon (Black, 1972; Black and Pepin, 1969) and xenon (Reynolds and Turner, 1964). Large anomalies in carbon (Halbout *et al*., 1986) and nitrogen (Lee, 1988) also suggested the presence of presolar grains. However, actual isolation of the grains required a lengthy procedure of tracking the carriers of isotopically anomalous noble gas components in primitive meteorites through numerous chemical dissolution and physical separation steps (Amari *et al*., 1994; Tang and Anders, 1988). This process, which has been termed 'burning down the haystack to find the needle' (Anders and Zinner, 1993) led to the identification of three carbonaceous presolar grain types: nanodiamonds (Lewis *et al*., 1987), silicon carbide (Bernatowicz *et al*., 1987) and graphite (Amari *et al*., 1990). Subsequent work on grains from acid residues led to the discovery of other presolar grain types, including spinel, corundum, hibonite, chromite and silicon nitride (see Zinner, 2014 for a comprehensive review).

Presolar silicates represent a special case. Although astronomical observations suggested the presence of abundant silicates in the circumstellar outflows of evolved O-rich stars (e.g., Waters *et al*., 1996; Demyk *et al*., 2000),

*Corresponding author (e-mail: floss@wustl.edu)

they were the last major type of presolar grain to be discovered. Their enhanced susceptibility to destruction, compared to other more refractory presolar phases, means that they are only found in the most primitive extraterrestrial samples, those that have largely escaped aqueous alteration and thermal metamorphism. Moreover, unlike most other presolar grain types, presolar silicates cannot be isolated by acid dissolution techniques because they are dissolved during this process along with the solar system silicates that dominate the meteorites in which presolar grains are found. Thus, the identification of presolar silicates requires a technique that can identify these tiny grains in situ or in physically disaggregated grain separates. Early efforts to identify presolar silicate grains in meteorites (Nittler, 1996; Messenger and Bernatowicz, 2000; Alexander *et al*., 2001) were unsuccessful, due to the difficulties associated with identifying a few anomalous grains in a sea of isotopically normal solar system silicates, compounded by the small (submicrometer) grain sizes expected of presolar silicates. With the advent of the NanoSIMS, and its unprecedented spatial resolution and high sensitivity, presolar silicate grains were first identified in interplanetary dust particles (IDPs) on the basis of their anomalous oxygen isotopic compositions (Messenger *et al*., 2003) and, shortly thereafter, were found in the carbonaceous chondrite Acfer 094 (Mostefaoui and Hoppe, 2004; Nguyen and Zinner, 2004; Nagashima *et al*., 2004).

Since these initial discoveries, coordinated micro-analytical techniques have provided a wealth of information about this group of presolar grains. Here we review what has been learned about and from presolar silicates since they were first discovered a little over ten years ago.

Analytical Methods

"Nothing tends so much to the advancement of knowledge as the application of a new instrument," noted the 19th century English chemist Sir Humphry Davy. Indeed, the development of new analytical instrumentation over the last 50 years, stimulated in large part by NASA's Apollo program, has led to profound advances in the fields of cosmochemistry, laboratory astrophysics and planetary science. Today the study of extraterrestrial materials encompasses a wide variety of different analytical techniques (Zinner *et al*., 2011) that continue to push the boundaries of our understanding of the formation and evolution of the solar system, the materials of which it is comprised and the time scales on which these events took place. The study of presolar silicates has benefited primarily from secondary ion mass spectrometry (SIMS), Auger spectroscopy, and transmission electron microscopy (TEM), each of which are discussed in more detail below.

Secondary Ion Mass Spectrometry (SIMS)

Although some early investigations (Nagashima *et al*., 2004, 2005; Kobayashi *et al*., 2005; Ebata *et al*., 2006; Tonotani *et al*., 2006) made use of a Cameca ims-1270 ion microprobe equipped with a SCAPS (stacked CMOS-type active pixel sensor) imaging device (Yurimoto *et al*., 2003), the majority of presolar silicate studies have used the raster ion imaging capabilities of the NanoSIMS 50 and 50L to identify these grains. While the details differ to some extent depending upon the laboratory and the type of material being studied (e.g., Messenger *et al*., 2003; Floss *et al*., 2006; Busemann *et al*., 2009; Floss and Stadermann, 2009; Vollmer *et al*., 2009a; Nguyen *et al*., 2010a; Leitner *et al*., 2012a; Nguyen and Messenger, 2014), the general procedure for these measurements involves rastering a Cs^+ primary ion beam (~100 nm diameter) over a small area (typically 10×10 or 20×20 μm^2) and collecting the secondary ions of the three oxygen isotopes ($^{16}O^-$, $^{17}O^-$, $^{18}O^-$) and secondary electrons. The NanoSIMS 50 allows the simultaneous collection of five species; common choices, in addition to oxygen, are $^{12}C^-$ and $^{13}C^-$ to allow for the identification of C-rich presolar grains such as SiC (e.g., Floss and Stadermann, 2009), or $^{28}Si^-$, $^{24}Mg^{16}O^-$ and/or $^{27}Al^{16}O^-$ to provide preliminary information about grain compositions (e.g., Vollmer *et al*., 2009a). The NanoSIMS 50L has seven detectors, which allows all silicon isotopes ($^{28}Si^-$, $^{29}Si^-$, $^{30}Si^-$) to be measured along with oxygen; alternatively, various combinations of the species listed above may be selected (e.g., Nguyen *et al*., 2010a; Nguyen and Messenger, 2014).

Measurements typically consist of multiple scans over the analysis area, which are then added together to form a single image measurement. Post-measurement image processing generally includes outlier removal and image alignment prior to calculation of isotope ratio images and identification of isotopically anomalous regions (Messenger *et al*., 2003; Floss and Stadermann, 2009; Nguyen *et al*., 2010a). Isotope mapping can be carried out in automated mode, with automatic stage movement to subsequent measurement areas, following a predefined grid pattern on the sample. The region of interest is typically pre-sputtered using a high beam current to implant Cs and, in the case of carbon-coated samples, to remove the carbon coat.

Presolar silicate searches have been carried out on a variety of samples prepared in various ways. Most commonly, fine-grained matrix areas identified in standard thin sections of primitive meteorites are analyzed (Floss and Stadermann, 2009; Vollmer *et al*., 2009a; Nguyen *et al*., 2010a; Leitner *et al*., 2012a). Alternatively, searches can be carried out on densely packed physically disaggregated grain size separates mounted on high purity Au foil (Nguyen, 2005; Nguyen and Zinner, 2004). Interplanetary dust particles and Antarctic

micrometeorites may be pressed into high purity Au (Messenger *et al*., 2003; Floss *et al*., 2006; Yada *et al*., 2008; Busemann *et al*., 2009) or ultra-microtomed and mounted on TEM grids (Messenger *et al*., 2005) or Si wafers (Floss *et al*., 2010) for analysis. Presolar silicate searches have also been carried out on impact craters in the Al foil collectors from the Stardust mission to comet Wild 2 (McKeegan *et al*., 2006; Stadermann *et al*., 2008; Leitner *et al*., 2010, 2012b; Floss *et al*., 2013) and in the 'aluminum kidney' of the Genesis spacecraft (Floss *et al*., 2015), although the topography of these craters presents some additional analytical challenges (Stadermann *et al*., 2008).

A problem common to most of the ion imaging searches to identify presolar silicates is that of signal dilution due to beam overlap onto surrounding isotopically normal grains. Nguyen *et al*. (2007) modeled the effects of raster imaging analysis on the compositions of isotopically anomalous grains and showed that dilution affected the isotopic compositions of all grains. The effects are greatest for grains with depletions in the minor isotopes of oxygen (^{17}O, ^{18}O). Dilution effects are also grain-size dependent, with the largest shifts observed for the smallest grains. Thus, the true isotopic composition of a presolar silicate identified in situ will always be more anomalous than its measured composition, although Nguyen *et al*. (2007) noted that the variety of factors influencing the degree of dilution precludes a determination of the original isotopic composition of any given grain.

The NanoSIMS is also used to carry out analyses of the Si, Mg and Fe isotopic compositions of presolar silicates. Silicon isotopes are typically measured with the Cs^+ primary beam, either subsequent to the O ion imaging searches with the NanoSIMS 50 (e.g., Mostefaoui and Hoppe, 2004; Vollmer *et al*., 2008; Yada *et al*., 2008; Leitner *et al*., 2012a) or together with the O isotopes, using the larger magnet of the NanoSIMS 50L (e.g., Nguyen *et al*., 2010a; Nguyen and Messenger, 2014). Measurements of the Mg and Fe isotopes in presolar silicate grains are complicated by the fact that these analyses are typically carried out with the O^- primary ion beam on the NanoSIMS. The diameter of the O^- beam is ~500 nm, larger than most presolar silicates, leading to significant problems with signal dilution from surrounding isotopically normal grains. FIB milling to isolate the grains prior to analysis is one approach to reducing contamination from surrounding isotopically normal silicates (Kodolányi *et al*., 2014; Nguyen and Messenger, 2014). An alternative approach that has been used for Fe is to measure the Fe isotopes as oxides, using the Cs^+ primary beam of the NanoSIMS (Vollmer and Hoppe, 2010; Ong *et al*., 2012; Ong and Floss, 2013, 2015). In addition to the improved spatial resolution, the ability to obtain secondary electron images greatly simplifies relocating the grains, particularly in meteorite thin sections. Because Fe is a major element in most presolar silicates (see below), measuring the Fe isotopes with the higher spatial resolution of the Cs^+ primary beam can be a viable alternative, despite the lower ion yields.

Auger spectroscopy

The isotopic composition of a presolar grain provides important information about its stellar origin (Nittler *et al*., 2008), but additional elemental and/or mineralogical information provides constraints on the conditions under which a grain condensed (e.g., Bernatowicz *et al*., 1996), and is necessary for comparison with astronomical data (Henning, 2009, 2010). Auger spectroscopy is a well-established surface analytical technique in the materials sciences (Watts and Wolstenholme, 2003), which takes advantage of the emission of electrons with characteristic energies (Auger electrons) from a sample irradiated by an electron beam. Like X-ray energies measured in an electron microprobe or scanning electron microscope, the kinetic energies of Auger electrons provide information about sample composition. The key difference between the two is the size of the analytical volume. Under typical measurement conditions, X-rays are emitted from a volume that is approximately 1 μm in diameter (Goldstein *et al*., 1992). In contrast, Auger electrons originate only from the top few nanometers directly under the electron beam (cf., figure 2 of Stadermann *et al*., 2009). The spatial resolution for Auger spectroscopy is, therefore, primarily dependent on the primary electron beam diameter and is on the order of tens of nanometers, ideally suited for the elemental characterization of presolar silicates, which typically have diameters of 200–300 nm.

Stadermann *et al*. (2009) provide a detailed overview of the development of Auger spectroscopy for the analysis of presolar grains. Briefly, Auger electron energy spectra are obtained with a 10 kV 0.25 nA primary electron beam, which is rastered over the grains of interest. Multiple spectral scans of a given grain are added together to obtain a single Auger spectrum, which is subjected to a 7-point Savitsky-Golay smoothing and differentiation routine prior to peak identification and quantification. Sensitivity factors for the major rock-forming elements (O, Si, Fe, Mg, Ca, and Al) have been determined from olivine and pyroxene standards of various compositions. These analytical protocols (low beam current, beam rastering, and repeated spectra acquisition) were established to reduce the possibility of electron beam damage on fragile presolar silicate grains, which can occasionally produce artifacts (e.g., compositional changes) in the Auger spectra (Stadermann *et al*., 2009). In addition to quantitative data from spectral measurements, high-resolution (10–20 nm) Auger elemental distribution maps can

provide detailed qualitative information about the distribution of elements within and around the grains of interest, such as the possible presence of rims and/or heterogeneities in the grains.

Auger spectroscopy has not found widespread application in the geosciences, due to problems with sample charging; because the technique is so surface sensitive, samples cannot be coated. However, as described by Stadermann *et al*. (2009), several factors contribute to the mitigation of this issue for the analysis of sub-micrometer presolar grains. Because the grains are typically much smaller than the electron stopping range of the primary beam energy used, most of the electrical charge is deposited outside of the grain of interest. This means that for samples deposited on a conductive surface, such as grain size separates on Au foil or ultra-microtome sections, the charge is immediately dissipated. For other samples, such as IDPs, Antarctic micrometeorites and meteorite thin sections, the grains tend to be embedded in a conductive C-rich matrix, again allowing for dissipation of the electrical charge. However, in some samples with C-poor matrix material, such as the enstatite chondrites, sample charging does prevent Auger analysis of presolar grains (Bose *et al*., 2010a).

While Auger spectroscopy is well-suited as a technique complementary to the NanoSIMS for the routine determination of the elemental compositions of presolar silicate grains, there are some limitations. Detection limits in Auger spectroscopy depend both on the element being analyzed and the overall noise level of the spectrum, but are typically around 3–5 at.%. Thus, although in principle all elements except for H and He can be measured with this technique, in practice it is limited to the determination of major element compositions. In addition, a number of factors, including signal-to-noise, sample charging and the presence of surface contamination, affect the quality of an Auger spectrum. While it is difficult to assign an actual uncertainty to the quantification of Auger spectra, based on these factors, Stadermann *et al*. (2009) provided relative errors (typically on the order of 10%) for the rock-forming elements based on the standard deviations of the Auger to electron microprobe ratios for these elements in the mineral standards used to obtain sensitivity factors. They noted, moreover, that compositional variations in the quantitative Auger measurements of 114 pyroxene and olivine standard grains followed Gaussian distributions about the nominal (Fe+Mg)/Si ratios of these minerals with some overlap at intermediate compositions (cf., figure 10 of Stadermann *et al*., 2009). Stadermann *et al*. (2009) concluded that 'while it may not always be possible on an individual grain basis to unequivocally distinguish between an olivine- and a pyroxene-like composition, on a statistical basis predominantly olivine-like grain populations will be markedly different from those that are dominated by pyroxene-like grains.'

Transmission electron microscopy (TEM)

Transmission electron microscopy provides elemental and structural information on a nanometer scale, and is, thus, ideal for the characterization of submicrometer-sized presolar grains. TEM analysis is carried out using high-energy electrons that are transmitted through the prepared sections. A variety of imaging techniques provide structural information about the samples, including bright-field (BF-TEM) imaging for determination of microstructures, high-resolution (HR-TEM) imaging for observing lattice structures and atomic planes, selected area electron diffraction (SAED) for crystal structure determination, and scanning TEM annular dark field (STEM-ADF) imaging for atomic number contrast. In addition, energy loss-filtered TEM (EF-TEM) can be used for elemental mapping, and energy dispersive X-ray spectroscopy (EDX) and electron energy loss spectroscopy (EELS) can be used to obtain compositional data; the latter also provides information about bond configurations and oxidation states.

Spatially correlated isotopic and elemental/structural measurements on the same samples provide the ideal analytical scheme for maximizing the information obtained from presolar grains. Such measurements have been done on ultramicrotome sections prepared from isolated presolar grains, by carrying out NanoSIMS measurements on the sections following TEM analysis (e.g., Croat *et al*., 2003, 2005; Stadermann *et al*., 2005). However, for presolar silicates identified in grain size separates, meteorite thin sections or particles pressed into a Au substrate, the grains must be extracted from their host matrix before TEM measurements can be carried out. This can be done by preparing cross-sectional slices from the material of interest through the use of a focused ion beam (FIB) cutout technique (Zega *et al*., 2007; Graham *et al*., 2008). Samples are typically prepared by initially depositing a Pt fiducial marker over the grain of interest for subsequent identification, followed by deposition of a rectangular mask over the area for protection from damage during ion milling. A Ga ion beam is then used to make trenches on either side of the region containing the grain. After attaching the section to a micromanipulator needle with a Pt weld, the remaining sides are cut away and the section is attached to a half-cut TEM grid, where it is thinned to electron transparency. Following TEM analysis, sections can also be returned to the NanoSIMS for additional isotopic measurements (Floss *et al*., 2014).

FIB-TEM is a labor-intensive technique and, thus, tends to be carried out only on select particularly interesting grains, but for many presolar silicates it is the only method that allows their detailed structural characteriza-

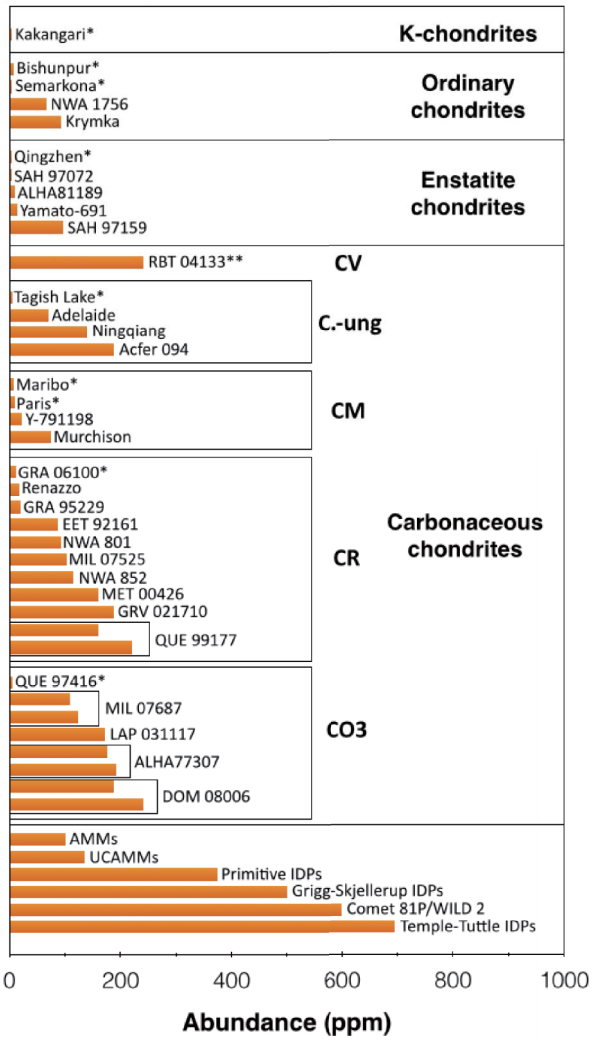

Fig. 1. Presolar silicate abundances in meteorites, Antarctic micrometeorites, interplanetary dust particles and samples from comet 81P/Wild 2. Single asterisks denote upper limits; double asterisk denotes unusually large error bars. Data sources: Bose et al. (2010a, 2012, 2014), Busemann et al. (2009), Davidson et al. (2014, 2015), Ebata et al. (2006), Floss and Stadermann (2009, 2012), Floss and Brearley (2014), Floss et al. (2006, 2010, 2012, 2013), Haenecour and Floss (2011), Haenecour et al. (2012, 2014a, 2015), Leitner et al. (2011, 2012a, 2012d, 2012e, 2013a, 2013b, 2014), Marhas et al. (2006), Mostefaoui (2011), Nguyen et al. (2007, 2010a), Nittler et al. (2013), Tonotani et al. (2006), Vollmer et al. (2009a), Zhao et al. (2010, 2011, 2013).

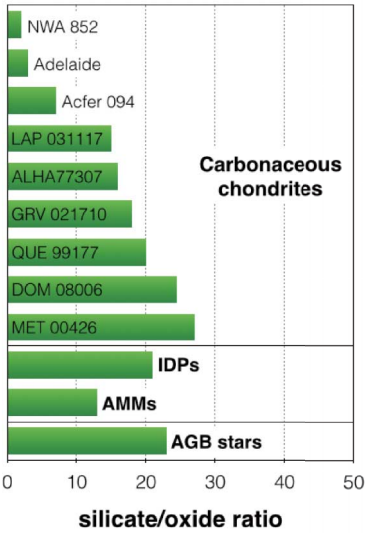

Fig. 2. Presolar silicate to oxide grain ratios in meteorites, Antarctic micrometeorites and interplanetary dust particles. The value for AGB stars is from Leitner et al. (2012a). Data sources: Bose et al. (2012), Floss and Stadermann (2009), Haenecour et al. (2014a, 2015), Leitner et al. (2012a), Nguyen et al. (2010a), Vollmer et al. (2009a), Yada et al. (2008), Zhao et al. (2013) and the Presolar Grain Database (Hynes and Gyngard, 2009).

tion (Vollmer *et al.*, 2007, 2009b, 2013; Busemann *et al.*, 2009; Stroud *et al.*, 2009, 2013, 2014; Nguyen *et al.*, 2010b, 2011, 2012, 2013, 2014). An alternate approach that has been applied successfully to IDPs involves creating ultramicrotome sections of entire particles for mineralogical characterization by TEM and NanoSIMS ion imaging searches to identify presolar grains (Messenger *et al.*, 2005; Keller and Messenger, 2011; Nguyen *et al.*, 2015).

Abundances

In the last ten years, more than 700 presolar silicate grains have been identified in primitive meteorites, IDPs and Antarctic micrometeorites, and they are the most abundant presolar grain type other than meteoritic nanodiamonds (Zinner, 2014). The abundance of these grains varies widely (Fig. 1), and is largely a reflection of the degree of secondary processing experienced by the material in which they are hosted. Abundances are highest in interplanetary dust particles, on the order of 400 ppm or more (Messenger *et al.*, 2003; Floss *et al.*, 2006, 2010; Busemann *et al.*, 2009), similar to the abundances inferred for samples from comet Wild 2 (Floss *et al.*, 2013). They are significantly lower in meteorites, indicating that even the most primitive of these samples have experienced more processing than IDPs. The bulk of presolar silicates have been found in carbonaceous chondrites, most notably CR3s and CO3s, as well as ungrouped C chondrites, such as Acfer 094. Maximum abundances in these meteorites are on the order of 200 ppm (Fig. 1). One of the defining characteristics common to primitive meteorites with high presolar grain abun-

dances is the presence of abundant fine-grained Fe- and Si-rich amorphous material in their matrices (e.g., Brearley, 1993; Greshake, 1997; Abreu and Brearley, 2010). As thermal metamorphism leads to recrystallization of the matrix and aqueous alteration leads to the formation of crystalline phyllosilicates in more processed meteorites, the abundance of presolar silicates decreases rapidly (e.g., Nagashima *et al*., 2005; Floss and Stadermann, 2012). Presolar silicates are present in some ordinary and enstatite chondrites, but maximum abundances are on the order of 100 ppm, lower than in carbonaceous chondrites. Similarly, presolar silicate abundances in Antarctic micrometeorites are around 100 ppm (Fig. 1).

The ratio of presolar silicates to oxides has also been interpreted to reflect the degree of sample processing (Fig. 2). Leitner *et al*. (2012a) calculated a theoretical value of ~23 for the silicate/oxide abundance ratio of dust from AGB stars. This is similar to the ratios observed in IDPs and the CR3 chondrites (Floss and Stadermann, 2009), suggesting that the presolar silicate and oxide abundances in these samples reflect their initial abundances in the regions of the solar nebula where the parent bodies of these samples formed. At the other end of the spectrum, the silicate/oxide ratios in the CR2 chondrite NWA 852 and the ungrouped carbonaceous chondrite Adelaide are only ~3, indicating the preferential destruction of presolar silicate grains in these meteorites through either parent body or nebular processing (Leitner *et al*., 2012a; Floss and Stadermann, 2012).

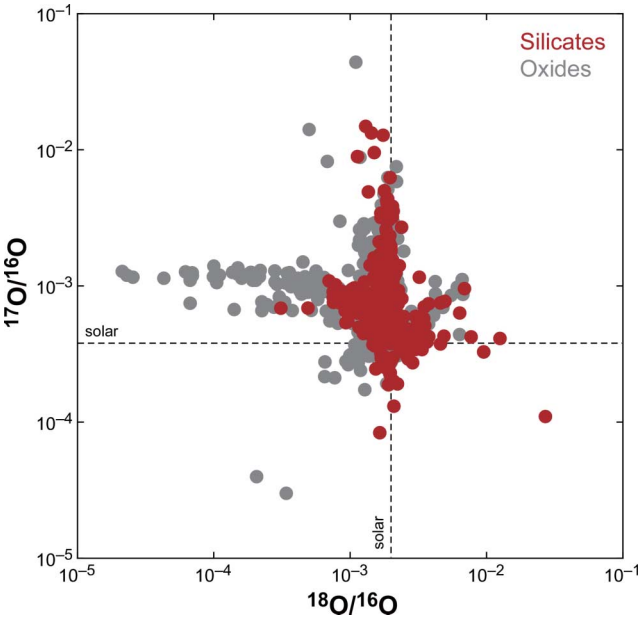

Fig. 3. Oxygen three isotope plot of presolar silicate grains (red) and presolar oxide grains (gray). Data sources: Bose et al. (2010a, 2012, 2014), Busemann et al. (2009), Choi et al. (1998, 1999), Davidson et al. (2014, 2015), Ebata et al. (2006), Floss and Stadermann (2009, 2012), Floss and Brearley (2014), Floss et al. (2006, 2010, 2012, 2013), Gyngard et al. (2010a, b), Haenecour and Floss (2011), Haenecour et al. (2012, 2014a), Huss et al. (1994), Keller and Messenger (2011), Leitner et al. (2011, 2012a, 2012d, 2012e, 2013a, 2013b, 2014), Marhas et al. (2006), Messenger et al. (2003, 2005), Mostefaoui and Hoppe (2004), Nagashima et al. (2004), Nguyen and Zinner (2004), Nguyen et al. (2003, 2007, 2010a), Nittler et al. (1994, 1997, 1998, 2008, 2013), Tonotani et al. (2006), Vollmer et al. (2009a), Yada et al. (2008), Zhao et al. (2010, 2011, 2013), Zinner et al. (2003, 2005) and the Presolar Grain Database (Hynes and Gyngard, 2009).

Isotopic Compositions

Oxygen isotopes

The oxygen isotopic compositions of presolar silicate grains are shown in Fig. 3, where they are compared to the compositions of presolar oxide grains (predominantly corundum and spinel). In earlier work on presolar oxides, Nittler *et al*. (1997) suggested division of the grains into four groups based on their isotopic compositions. Although the boundaries between the groups are somewhat fluid and not all grains fit neatly into one category, the classification scheme does provide general information about the stellar sources of the grains. As is evident from Fig. 3, the distribution of presolar silicate grains is broadly similar to that of the oxides.

Group 1 grains are characterized by enrichments in ^{17}O and solar to slightly sub-solar $^{18}O/^{16}O$ ratios, and are thought to have originated in oxygen-rich low-mass red giant and asymptotic giant branch (AGB) stars (Huss *et al*., 1994; Nittler *et al*., 1997). The evolution of low-to-intermediate mass AGB stars has been reviewed in detail by Nitttler *et al*. (2008) and Karakas and Lattanzio (2014), and we provide only a brief overview here. Hydrogen burning during the CNO cycles in the inner layers of the star results in the production of ^{17}O and the destruction of ^{18}O (Boothroyd and Sackman, 1999). As the star enters the red giant phase, this material is dredged up to the envelope of the star (first dredge-up) where grain formation takes place, resulting in grains with enhanced $^{17}O/^{16}O$ ratios. The $^{18}O/^{16}O$ ratios remain largely unchanged relative to the star's initial composition, indicating that the bulk of these grains originated in stars with initial metallicities close to solar. Group 3 grains with depletions in ^{17}O and ^{18}O (Fig. 3) likely also have red giant or AGB origins, but must have formed in stars with metallicities significantly less than solar (Nittler *et al*., 2008).

Boothroyd and Sackman (1999) calculated a limit on the degree of ^{17}O enrichment due to dredge-up in low to intermediate mass stars of close-to-solar metallicity, with a maximum $^{17}O/^{16}O$ ratio of about 4×10^{-3}. Newer calcu-

lations with a revised estimate of solar metallicity and new reaction rates suggest somewhat higher limits of approximately 6×10^{-3} (Gyngard *et al*., 2011). Thus, dredge-up in red giant and AGB stars cannot account for the isotopic compositions of Group 1 grains with very high $^{17}O/^{16}O$ ratios, often termed 'extreme Group 1 grains' (Vollmer *et al*., 2008). Nittler and Hoppe (2005) suggested that such grains could have a nova origin. However, model calculations show that the predicted isotopic compositions for pure nova ejecta are much more anomalous than the grain data, requiring extensive dilution with isotopically close-to-solar material to reproduce the grain compositions (Vollmer *et al*., 2008; Gyngard *et al*., 2010a, 2010b, 2011; Leitner *et al*., 2012c; Nguyen and Messenger, 2014). Another possibility, suggested by Nittler *et al*. (2008), is that mass loss to a binary companion could reduce the envelope of a main sequence star, with the result that the ^{17}O brought up during the first dredge-up is less diluted, leading to higher $^{17}O/^{16}O$ ratios. In either case, more modeling is clearly needed to understand the origins of these grains.

Group 2 grains also have elevated $^{17}O/^{16}O$ ratios, but they are far more depleted in ^{18}O than can be accounted for by the first dredge-up. It has been suggested that these grains experienced extra mixing in the AGB phase, known as 'cool bottom processing' (Wasserburg *et al*., 1995; Nollett *et al*., 2003), in which material from the star's envelope slowly circulates through hot regions near the H shell, resulting in additional destruction of ^{18}O. This process also produces the short-lived radionuclide ^{26}Al (Nollett *et al*., 2003) and, thus, measurement of the Mg isotopes to look for excesses in the decay product ^{26}Mg can provide additional evidence that a grain's composition has been affected by cool bottom processing (Nguyen and Zinner, 2004; Nittler *et al*., 2008).

Finally, Group 4 grains show enrichments in ^{18}O, with or without accompanying enrichments in ^{17}O (Fig. 3). The origin of these grains has been unclear (Nittler *et al*., 1997), but recent work has favored an origin in the ejecta of type II supernovae (e.g., Messenger *et al*., 2005; Nittler *et al*., 2008; Nguyen and Messenger, 2014), in which the enrichments in ^{18}O are thought to be produced from partial He burning in the He/C zone of these massive stars. Nittler (2007) noted that the isotopic compositions of those Group 4 grains in which the ^{18}O excesses are associated with corresponding ^{17}O enrichments of similar magnitude could be reproduced by mixing variable amounts of material from the ^{16}O-rich inner zones with a single mixture of the H envelope and the ^{18}O-rich He/C zone. Notably, this mixing line also passes near some ^{16}O-rich Group 3 grains that are not well-explained by an AGB origin (Nittler *et al*., 2008).

Although the isotopic compositions of presolar silicate grains are represented by the same major groups as those of presolar oxides, Fig. 3 shows that in detail there are some differences. The majority of both oxide and silicate grains belong to Group 1. However, while the ^{18}O-depleted Group 2 grains are well represented in the presolar oxide population, relatively few presolar silicates belong to Group 2. Similarly, Group 3 grains, with depletions in ^{18}O and ^{17}O, are also underrepresented among the presolar silicates compared to oxides. These differences can be attributed to two biases in the analytical techniques used to identify the grains. First, some presolar oxide grains were identified by ion imaging searches of acid residue separates carried out by the older 'f series' Cameca ion microprobes (e.g., Nittler, 1996). Due to the lower sensitivity of these instruments and the difficulty of measuring ^{17}O, the least abundant oxygen isotope, grains were typically identified by low mass resolution imaging of $^{18}O/^{16}O$ ratios (Nittler *et al*., 1997), leading to an overrepresentation of grains with ^{18}O anomalies, relative to those with ^{17}O anomalies.

Although all three oxygen isotopes are measured in the NanoSIMS ion imaging searches used to identify most presolar silicates, analytical biases are also an issue. Because these measurements are carried out in situ, and the presolar silicates are usually surrounded by isotopically normal O-rich grains, isotope dilution is a significant problem. Nguyen *et al*. (2007) modeled the effects of raster ion imaging analysis on the compositions of isotopically anomalous grains surrounded by isotopically normal grains, and showed that dilution effects were observed for all grain compositions. These dilution effects are grain-size dependent, with the largest shifts toward normal compositions observed for the smallest grains. The simulations of Nguyen *et al*. (2007) suggest that for grains similar in size to most presolar silicates (~250 nm) the effects of isotopic dilution will shift grain compositions to such an extent that almost half of all grains will not be identified as presolar in raster imaging measurements. Isotopic dilution is most pronounced for grains with depletions in the minor oxygen isotopes, such as Group 3 grains with depletions in $^{17,18}O$. Similarly, some Group 2 grains may be misidentified as Group 1 grains.

Group 4 grains also show differences between the distributions of oxides and silicates. While both silicates and oxides are represented among Group 4 grains with similar enrichments in ^{17}O and ^{18}O, oxide grains with ^{18}O enrichments that are not accompanied by ^{17}O excesses appear to be underrepresented compared to silicates. Both types of Group 4 grains have likely supernova origins, and this difference may reflect a difference in condensation environments between oxides and silicates. Another unusual feature of the Group 4 grains was first noted by Yada *et al*. (2008), who observed that IDPs and Antarctic micrometeorites (AMMs) have a higher proportion of Group 4 grains than primitive carbonaceous chondrites.

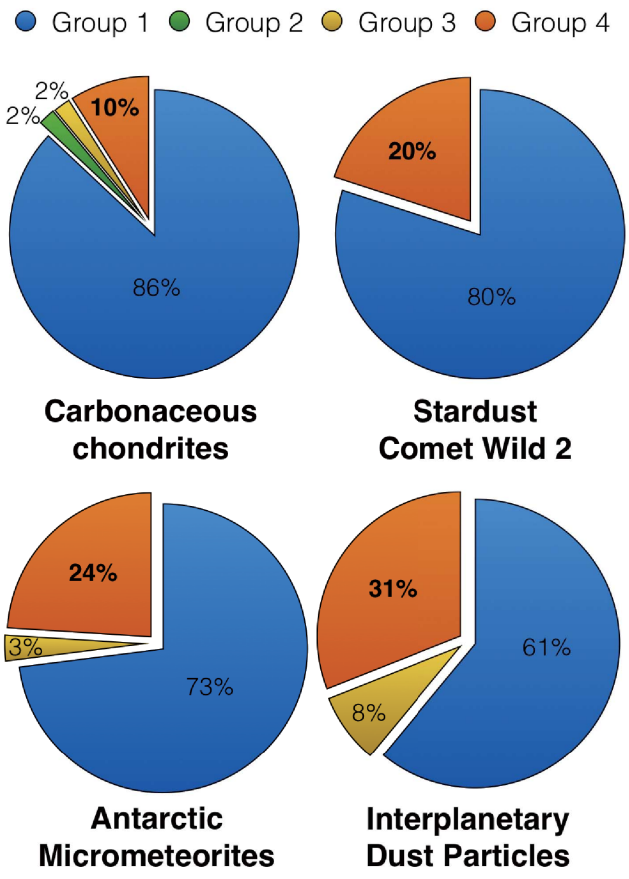

Fig. 4. Distribution of the isotopic compositions of O-rich presolar grains in meteorites, IDPs, AMMs and samples from comet Wild 2. The fraction of Group 4 grains is significantly smaller in carbonaceous chondrites than in other extraterrestrial samples.

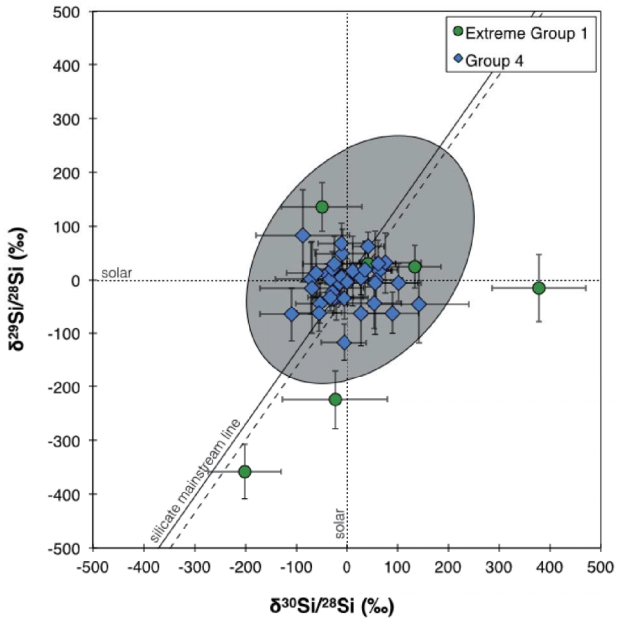

Fig. 5. Silicon three isotope ($^{30}Si/^{28}Si$ and $^{29}Si/^{28}Si$ plotted as permil deviations from normal) plot of presolar silicate grains. Group 1 grains are shown by the shaded ellipse and define a correlation line that is parallel to but slightly offset from the SiC mainstream line (dashed line). Data sources: Busemann et al. (2009), Leitner et al. (2012a), Mostefaoui and Hoppe (2004), Nagashima et al. (2004), Nguyen and Messenger (2014), Nguyen et al. (2007, 2010a), Vollmer et al. (2008), Yada et al. (2008), and the Presolar Grain Database (Hynes and Gyngard, 2009).

Haenecour *et al*. (2012) confirmed this observation with additional data on Antarctic micrometeorites. Figure 4 shows that Group 4 grains make up 25–30% of the presolar silicate/oxide population in IDPs and AMMs, but only 10% of the population in primitive carbonaceous chondrites. The O-rich presolar grains from comet Wild 2 appear to have a distribution similar to that of IDPs and AMMs, but with only five grains found to date (Stadermann *et al*., 2008; Leitner *et al*., 2010; Floss *et al*., 2013), the significance of this result is uncertain. Only grains identified by NanoSIMS raster ion imaging are included in this breakdown; thus, analytical biases like those discussed above do not explain the difference. One possible explanation is suggested by the fact that the oxygen isotopic compositions of many Group 4 grains lie on a single mixing line, suggesting that they may have originated from a single supernova source that injected material into the early solar nebula (Nittler, 2007; Nittler *et al*., 2008). A similar model has been invoked to account for the presence of short-lived radionuclides in early solar system materials (Huss *et al*., 2009; Ouellette *et al*., 2009, 2010). If most Group 4 grains did form in a single nearby supernova, the heterogeneity in their distribution among AMMs, IDPs and primitive meteorites would reflect formation of these materials in different parts of the solar nebula with different abundances of Group 4 grains, or at different times during solar system formation (Yada *et al*., 2008; Haenecour *et al*., 2012).

Silicon isotopes

Close to 200 presolar silicate grains have been measured for their Si isotopic compositions (Nagashima *et al*., 2004; Mostefaoui and Hoppe, 2004; Messenger *et al*., 2005; Nguyen *et al*., 2007, 2010a; Yada *et al*., 2008; Vollmer *et al*., 2008; Busemann *et al*., 2009; Leitner *et al*., 2012a; Nguyen and Messenger, 2014). In a three-isotope plot, the Si isotopic compositions of Group 1 and Group 2 presolar silicates generally fall along a correlation line defined by presolar mainstream SiC grains of AGB origin (Fig. 5), but are systematically depleted in

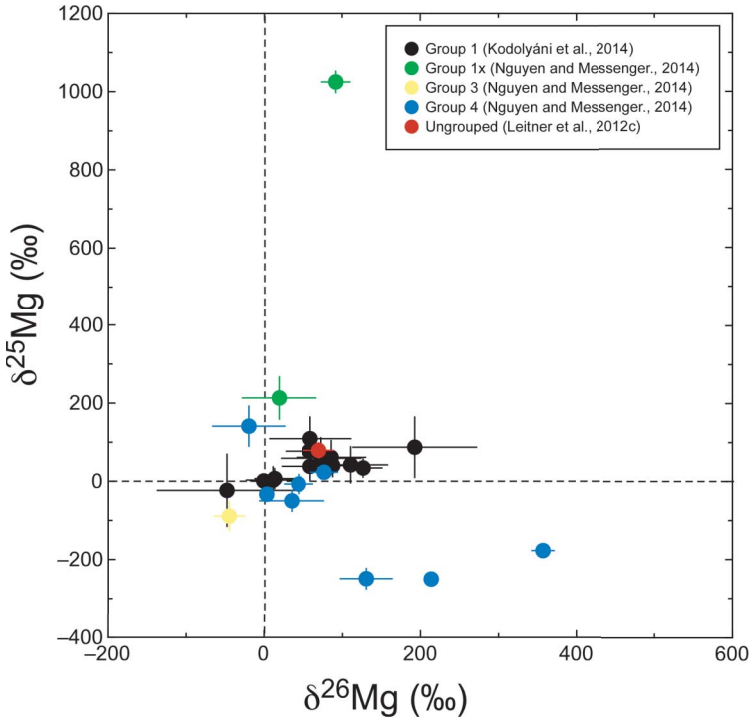

Fig. 6. Magnesium three-isotope ($^{26}Mg/^{24}Mg$ and $^{25}Mg/^{24}Mg$ plotted as permil deviations from normal) plot of O-anomalous grains from Acfer 094 (Leitner et al., 2012c; Kodolányi et al., 2014; Nguyen and Messenger, 2014). Errors are 1σ.

^{30}Si (Mostefaoui and Hoppe, 2004; Vollmer *et al*., 2008; Nguyen *et al*., 2010a). The mainstream SiC correlation line reflects the effects of galactic chemical evolution and the varying initial compositions of the stellar sources of these grains (Zinner *et al*., 2006), with minor contributions to ^{29}Si (~10‰) and ^{30}Si (~30‰) from neutron capture reactions and dredge-up during the AGB phase. These neutron capture products don't significantly affect the star's surface composition until it becomes C-rich (Zinner *et al*., 2006) and are not expected to contribute to the Si isotopic compositions of presolar silicates, which therefore should more closely reflect the metallicities of their parent stars (Nguyen *et al*., 2007, 2010a). However, Nguyen *et al*. (2010a) investigated the effect of isotopic dilution on Si isotopes in presolar silicates and concluded that most of the data obtained to date are too strongly affected by dilution to provide meaningful constraints on galactic chemical evolution.

The number of Group 4 presolar silicates for which Si isotopic data are available is still limited. Some grains exhibit enrichments in ^{28}Si, qualitatively similar to SiC X grains, which originate in the ejecta of type II supernovae (Vollmer *et al*., 2008), while others have normal ^{30}Si/^{28}Si ratios and normal or depleted ^{29}Si/^{28}Si ratios (Messenger *et al*., 2005; Bland *et al*., 2007; Nguyen and Messenger, 2014). Finally, the Si isotopes of several extreme Group 1 grains have enhanced ^{30}Si/^{28}Si ratios (Vollmer *et al*., 2008; Leitner *et al*., 2012c; Nguyen and Messenger, 2014) and one grain is enriched in ^{29}Si (Nguyen and Messenger, 2014), qualitatively consistent with predictions from nova models. As noted above for the oxygen isotopes, however, extensive dilution with isotopically normal material is required to reproduce the grain compositions.

Magnesium isotopes

Relatively few Mg isotopic measurements have been carried out on presolar silicates. The Mg isotopes of several Group 1 silicates (Fig. 6) have close-to-solar compositions similar to those of Group 1 oxides, with little to no evidence of contributions from the decay of ^{26}Al (Kodolányi and Hoppe, 2011a, b; Kodolányi *et al*., 2014), as does a Group 3 silicate measured by Nguyen and Messenger (2014). Stellar evolution models predict little increase in ^{25}Mg and ^{26}Mg in the envelopes of low-mass AGB stars compared to their initial ratios (Palmerini *et al*., 2011) and, thus, the grain compositions likely reflect galactic chemical evolution.

The Mg isotopic compositions of two extreme Group 1 silicates measured by Nguyen and Messenger (2014) show enrichments in ^{25}Mg (1025 ± 29‰ and 92 ± 19‰; Fig. 6). As for the O and Si isotopes, these grain compositions can be reproduced by dilution of nova material. A nova origin was also suggested for a presolar silicate from

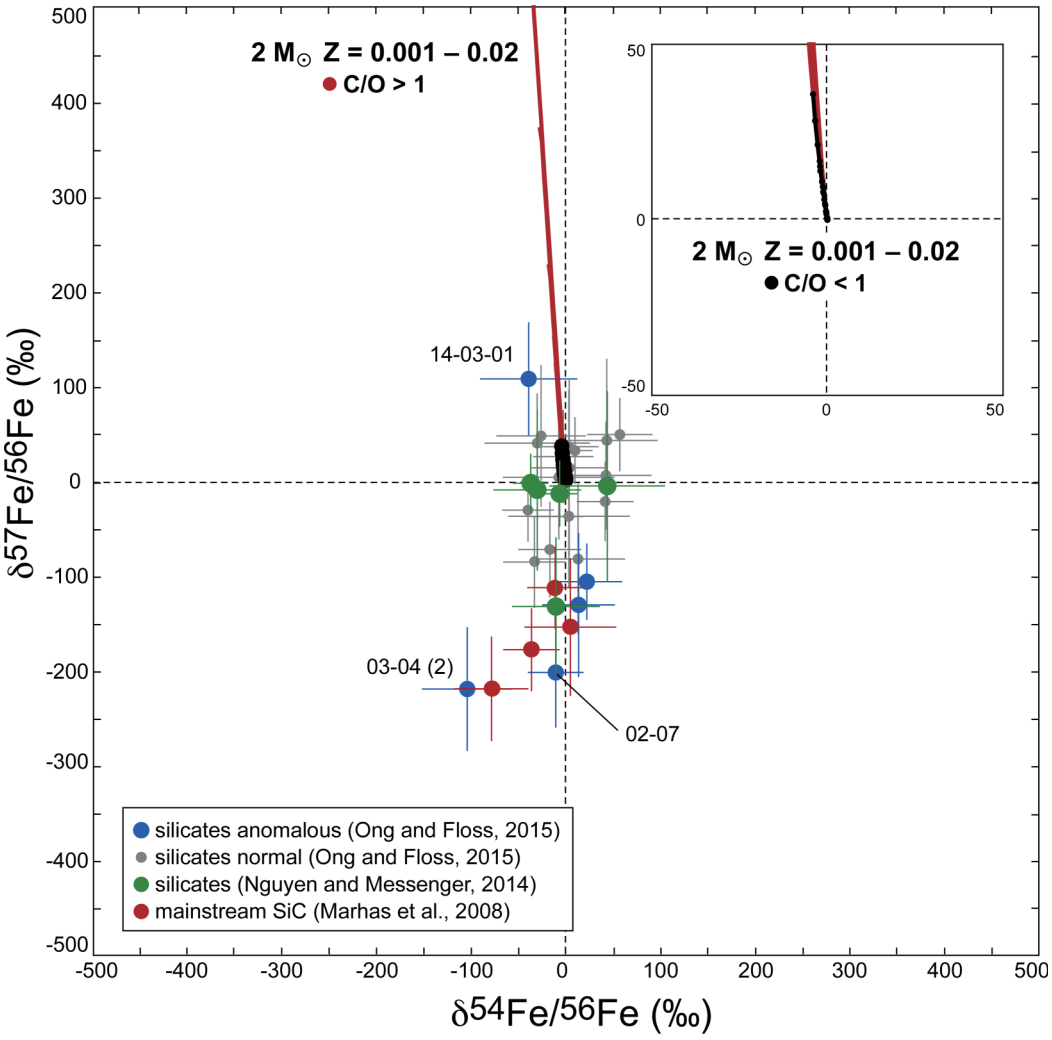

Fig. 7. Iron three-isotope ($^{54}Fe/^{56}Fe$ and $^{57}Fe/^{56}Fe$ plotted as permil deviations from normal) plot of O-anomalous grains from Acfer 094 (Nguyen and Messenger, 2014; Ong and Floss, 2015) and mainstream SiC grains from Murchison (Marhas et al., 2008). Errors are 1σ. Also shown are model predictions for 2 $M_\odot$ AGB stars with metallicities from 0.001 to 0.02 (Cristallo et al., 2011). See text for details.

GRA 95229 with modest enhancements in ^{25}Mg and ^{26}Mg (Leitner *et al.*, 2012c).

Nguyen and Messenger (2014) also measured the Mg isotopic compositions of a number of Group 4 silicate grains (Fig. 6). Several of the grains have solar $^{25}Mg/^{24}Mg$ and $^{26}Mg/^{24}Mg$ ratios, while others are depleted in ^{25}Mg and enriched in ^{26}Mg. For two grains with O isotopic compositions above the GCE line, Nguyen and Messenger (2014) evaluated and ruled out a high metallicity AGB origin, because the grains did not show the expected enrichments in ^{25}Mg. Instead, they found that the Mg isotopic compositions of all of the grains can be reproduced by mixing various zones of a 15 $M_\odot$ supernova model (Rauscher *et al.*, 2002).

Finally, excess ^{26}Mg, attributed to the decay of ^{26}Al, was observed in a Group 2 silicate measured by Nguyen and Zinner (2004). The inferred initial $^{26}Al/^{27}Al$ of this grain is ~0.12, higher than that of any presolar oxide grains measured to date. Cool bottom processing in low-mass thermally pulsing AGB stars, which has been invoked to account for the ^{18}O depletions of Group 2 grains, also produces ^{26}Al (Wasserburg *et al.*, 1995). The $^{26}Al/^{27}Al$ ratio is dependent on the temperature experienced by the circulated material, which in turn depends on the depth of penetration (Nollett *et al.*, 2003). The high $^{26}Al/^{27}Al$ ratio of this grain requires very deep mixing, but can be accounted for if the envelope material is circulated to regions with temperatures of ~50 × 10^6 K or more (Nguyen and Zinner, 2004; Nittler *et al.*, 2008).

Iron isotopes

Most of the grains measured to date for Fe isotopes have $^{54}Fe/^{56}Fe$ and $^{57}Fe/^{56}Fe$ ratios that are consistent with solar within errors (Nguyen and Messenger, 2014; Ong and Floss, 2015), but several grains with anomalous isotopic compositions have also been observed (Fig. 7). All but one of the isotopically anomalous grains belong to Group 1, with origins in low-mass red giant or AGB stars. For the Fe isotopes, the largest compositional changes take place during the AGB phase, when thermal pulses drive nucleosynthesis and convective mixing episodes bring newly synthesized material to the star's surface. Cristallo *et al*. (2011) systematically investigated the evolution of low-mass AGB stars and calculated stellar yields for a series of masses and metallicities. Neutron capture in the He intershell, from either the $^{13}C(a,n)^{16}O$ or $^{22}Ne(a,n)^{25}Mg$ neutron sources leads to the destruction of ^{54}Fe and ^{56}Fe, and the production of ^{57}Fe and ^{58}Fe. Thus, $^{54}Fe/^{56}Fe$ ratios are not expected to change substantially from the initial values of the parent stars, whereas the $^{57}Fe/^{56}Fe$ and $^{58}Fe/^{56}Fe$ ratios will be elevated, with maximum enrichments of up to ~700‰ for ^{57}Fe (Fig. 7). However, in the early dredge-up episodes where the C/O ratios are <1 and O-rich grains are more likely to form, the maximum enrichments in ^{57}Fe are less, on the order of about 50‰. Thus, within errors, the normal $^{54}Fe/^{56}Fe$ and $^{57}Fe/^{56}Fe$ ratios of most of the grains are consistent with these model predictions. However, several grains show depletions in ^{57}Fe (Fig. 7), which are not consistent with current AGB models. Four mainstream SiC grains of AGB origin also show deficits in ^{57}Fe like those observed in the silicates (Marhas *et al*., 2008). The isotopic compositions of these grains remain unexplained.

A Group 3 silicate grain analyzed by Nguyen and Messenger (2014) also shows a depletion in ^{57}Fe similar in magnitude to that observed for the Group 1 silicates and mainstream SiC discussed above (Fig. 7), although the errors on the measurement are large. These authors favored a supernova origin for the grain, but noted that an origin from a metal-poor star could not be excluded given uncertainties in GCE and AGB models.

Elemental Compositions

Ferromagnesian silicates

The elemental compositions of over 400 O-rich presolar grains identified by NanoSIMS raster ion imaging have been measured by Auger spectroscopy (Floss and Stadermann, 2009, 2012; Vollmer *et al*., 2009a; Bose *et al*., 2010a, 2010b, 2012; Nguyen *et al*., 2010a; Zhao *et al*., 2013). The vast majority of the grains analyzed are ferromagnesian silicates; grains that contain Ca and/or Al (above the detection limits of the Auger Nanoprobe) are relatively rare. Based on elemental ratios of

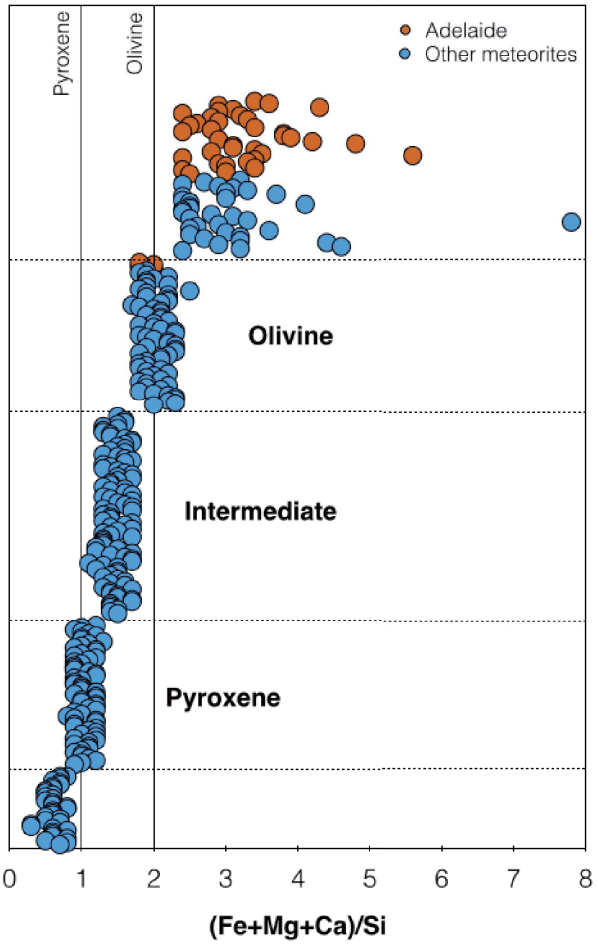

Fig. 8. Plot of (Fe+Mg+Ca)/Si ratios in presolar ferromagnesian silicate grains. Data sources: Floss and Stadermann (2009, 2012), Vollmer et al. (2009a), Bose et al. (2010a, 2010b, 2012), Nguyen et al. (2010a), Zhao et al. (2013).

(Fe+Mg+Ca)/Si (Fig. 8), it is apparent that most of the grains have stoichiometries consistent with either olivine (Fe+Mg/Si = 2) or pyroxene (Fe+Mg+Ca/Si = 1), each comprising 20% of the presolar silicate population, or have compositions that are intermediate between these (30 % of the population). The fraction of grains with intermediate (Fe+Mg+Ca)/Si ratios is significantly higher than expected based on the Gaussian distribution of these ratios observed in the Auger measurements of olivine and pyroxene standards (Stadermann *et al*., 2009), indicating that this is a statistically significant presolar grain population, and not an artifact of the measurement technique.

In addition to the intermediate grains, a number of other presolar silicates have non-stoichiometric compositions, with (Fe+Mg+Ca)/Si ratios that are less than 1 or greater than 2 (grains from the meteorite Adelaide shown in Fig. 8 represent a special case and are discussed in

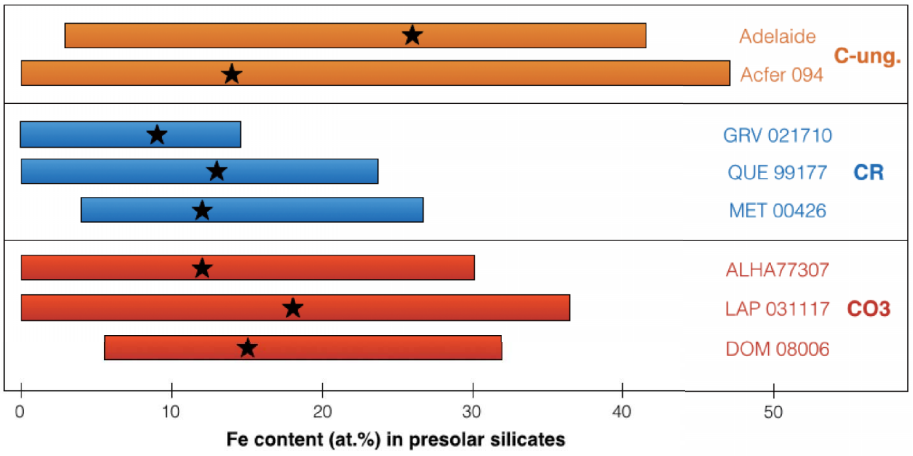

Fig. 9. Range of Fe concentrations in presolar silicate grains from primitive carbonaceous chondrites. Stars show the median value for the grains from each meteorite. Data sources: Floss and Stadermann (2009, 2012), Bose et al. (2010a, 2012), Nguyen et al. (2010a), Vollmer et al. (2009a), Zhao et al. (2013), Haenecour and Floss (2012), Haenecour et al. (2015).

more detail below). Several explanations have been proposed for the non-stoichiometric nature of many of the presolar silicate grains. Irradiation, shock and sputtering processes in the interstellar medium can induce changes in the structures, chemical compositions and porosities of the grains (Demyk *et al*., 2001; Carrez *et al*., 2002), and may play a role in transforming stoichiometric grains into grains with non-stoichiometric compositions (Min *et al*., 2007; Keller and Messenger, 2011). Alternatively, non-stoichiometric compositions may be primary, the result of condensation under kinetic (i.e., non-equilibrium) conditions. This is consistent with modeling work on the formation of dust in O-rich stars, which suggests that most silicate dust forms during short high mass-loss episodes that occur after thermal pulses in thermally pulsing AGB stars (Gail *et al*., 2009). The stellar environment during these episodes will be highly variable, with strong stellar winds and rapid temperature drops, leading to grain formation under kinetic conditions.

Bose *et al*. (2012) noted that Group 4 grains contain a significantly higher proportion of grains with olivine compositions than Groups 1 and 2 grains. Grain lifetimes in the interstellar medium are shorter than the rate at which grains are replenished from stellar sources (Tielens, 1998). If Group 4 grains were, in fact, injected into the early solar nebula by a nearby supernova, as discussed above, these grains would likely have been incorporated into primitive solar system materials before alteration of their compositions and/or structures through irradiation and sputtering processes in the ISM. This would imply that the high proportion of olivine compositions among Group 4 grains reflects initial relative abundances at the time of incorporation into the solar nebula. Grains from Groups 1 and 2, in contrast, are more likely to reflect a combination of initial grain compositions and changes due to secondary processing as the grains traverse the ISM.

Auger Nanoprobe studies have also shown that presolar silicates have high (and variable) Fe concentrations (Fig. 9), whereas stellar observations (e.g., Demyk *et al*., 2000; Min *et al*., 2007) and thermodynamic calculations (e.g., Lodders and Fegley, 1999) predict Mg-rich compositions. Possible scenarios to account for the high Fe abundances have been discussed extensively in the literature (Floss and Stadermann, 2009; Vollmer *et al*., 2009a; Nguyen *et al*., 2007, 2010a; Bose *et al*., 2010b). Secondary alteration has played a role in some meteorites, as discussed in more detail below. However, most of the meteorites with high presolar silicate abundances show little evidence of alteration. Thus, it seems likely that much of the Fe seen in the grains is primary, with the elevated Fe abundances probably due to kinetic condensation of the grains in the stellar envelopes where they formed (Gail and Sedlmayr, 1999; Ferrarotti and Gail, 2001). The modeling work of Gail *et al*. (2009) suggests that silicate dust should consist of a mixture of olivine and pyroxene, with an average mole fraction of the Mg-rich component of about 0.6, consistent with the Fe-rich compositions of many of the presolar silicates.

GEMS (Glass with Embedded Metal and Sulfides)

GEMS are nanometer-sized (100–500 nm) aggregates of amorphous ferromagnesian silicates with abundant kamacite and Fe-Ni sulfide subgrains (Bradley, 1994a; Keller and Messenger, 2011). They are commonly found in chondritic porous (CP) IDPs (Bradley, 1994a, 1994b; Bradley and Dai, 2004; Keller and Messenger, 2011), and have also been identified in ultra-carbonaceous Antarctic micrometeorites (UCAMMs, Dobrica *et al*., 2012;

Noguchi *et al*., 2008). Ishii *et al*. (2008) identified GEMS-like objects in some Stardust tracks; however their bulk compositions differ substantially from those of GEMS found in IDPs.

While a small fraction of all GEMS (about 6%) have a clear circumstellar origin, with anomalous O isotopic compositions similar to those observed in presolar silicate grains, the vast majority have O isotopic compositions consistent with solar values (Stadermann and Bradley, 2003; Keller and Messenger, 2011). The formation processes of GEMS are still debated, with two main hypotheses. Bradley (1994a, 2013) proposes that GEMS are the result of space weathering of free-floating circumstellar grains by extensive irradiation in the interstellar medium (ISM). In contrast, Keller and Messenger (2011, 2013) suggest that GEMS have both presolar and solar nebula origins: isotopically anomalous GEMS formed in stellar envelope or ejecta while isotopically solar GEMS formed by non-equilibrium condensation in the solar nebula. Keller and Messenger (2011) argue that the large chemical variations observed in GEMS are inconsistent with a formation of these grains by extensive homogenization of chemical and isotopic compositions of circumstellar silicates in the ISM, as proposed by Bradley (1994a).

To date GEMS have not been definitively identified in meteorites. GEMS show large variations in bulk composition, with (Fe+Mg+Ca)/Si ratios that span the ranges observed in presolar silicate grains (cf., figure 7 in Keller and Messenger, 2011) suggesting that some presolar silicates may be GEMS-like objects. Given the limited number of presolar silicates studied with TEM, it is possible that GEMS are present in the presolar silicate population (e.g., Vollmer *et al*., 2009b), but have not yet been recognized. One complication is that most meteorites seem to have experienced more secondary alteration than primitive anhydrous IDPs, leading to compositional alterations; indeed Vollmer *et al*. (2009a, b) noted that presolar silicates are depleted in S and contain few nanophase Fe metal particles compared to GEMS from IDPs. Thus, if GEMS are a significant component in meteorites (whether of circumstellar or solar system origin), they may be difficult to recognize.

SiO_2

Auger spectroscopy has led to the identification of several grains with stoichiometries consistent with SiO_2 (Floss and Stadermann, 2009; Nguyen *et al*., 2010a; Bose *et al*., 2012; Haenecour *et al*., 2013a). Most of these grains have isotopic compositions consistent with origins in low-mass AGB stars, but two are Group 4 grains with likely origins in the ejecta of type II supernovae (Haenecour *et al*., 2013a). Theoretical considerations indicate that silica can condense in stellar winds under non-equilibrium conditions when only part of the gas phase SiO is consumed by the formation of Mg-Fe-silicates. This may occur in stars with low Mg/Si ratios and low mass-loss rates (Gail and Sedlmayr, 1999; Ferrarotti and Gail, 2001). Moreover, experimental work has shown that non-equilibrium condensation does produce silica aggregates, specifically tridymite (Rietmeijer *et al*., 2009). Attempts at mineralogical characterization of presolar SiO_2 grains have been unsuccessful so far, largely due to the very small sizes of these grains (e.g., Bose *et al*., 2012). However, these initial observations suggest that if crystalline silica does condense in stellar environments, it may be more likely to do so as the high-temperature polymorphs tridymite and cristobalite, than as quartz.

Composite grains

Theoretical models suggest that grain condensation is facilitated by the presence of seed nuclei upon which thermodynamically stable phases can condense and that refractory oxides, such as Al_2O_3 or TiO_2, may serve as seed nuclei for the condensation of presolar silicate minerals (Gail and Sedlmayr, 1999; Sogawa and Kozasa, 1999). Composite presolar grains that consist of aggregates of compositionally distinct subgrains (Vollmer *et al*., 2009a; Nguyen *et al*., 2010a, 2014; Floss and Stadermann, 2012; Bose *et al*., 2012; Stroud *et al*., 2013; Leitner *et al*., 2012a, 2014) have been identified and, in some cases, Al-rich oxides are associated with ferromagnesian silicates, indicating compositional evolution of the stellar environment (Vollmer *et al*., 2009a; Floss and Stadermann, 2012; Leitner *et al*., 2014; Nguyen *et al*., 2014). Figure 10 shows a striking example from the Krymka LL chondrite. This Group 1 grain is large, about 800 × 3,750 nm, and consists of a central Al-rich core surrounded by a Si-rich mantle (Leitner *et al*., 2014). The Al-rich core also contains Ca and Ti, but no Fe or Mg. The mantle surrounding this core appears to be a complex mixture of multiple compositionally distinct grains. Some grains are Fe-rich, with minor amounts of Mg, while others appear to consist only of Si and O. Calcium and Ti are also present in parts of the mantle.

In many cases, the oxygen isotopic compositions of these composite grains are uniform, indicating that, despite the difference in elemental compositions, there was no substantial change in the oxygen isotopic composition of the gas during condensation of these components (Vollmer *et al*., 2009a; Bose *et al*., 2012; Floss and Stadermann, 2012). For those grains in which oxygen isotopic compositions differ among different components of the composite grain, the differences have been attributed either to signal dilution from surrounding isotopically normal material (Vollmer *et al*., 2009a; Leitner *et al*., 2012a) or partial re-equilibration during secondary processing (Floss and Stadermann, 2012).

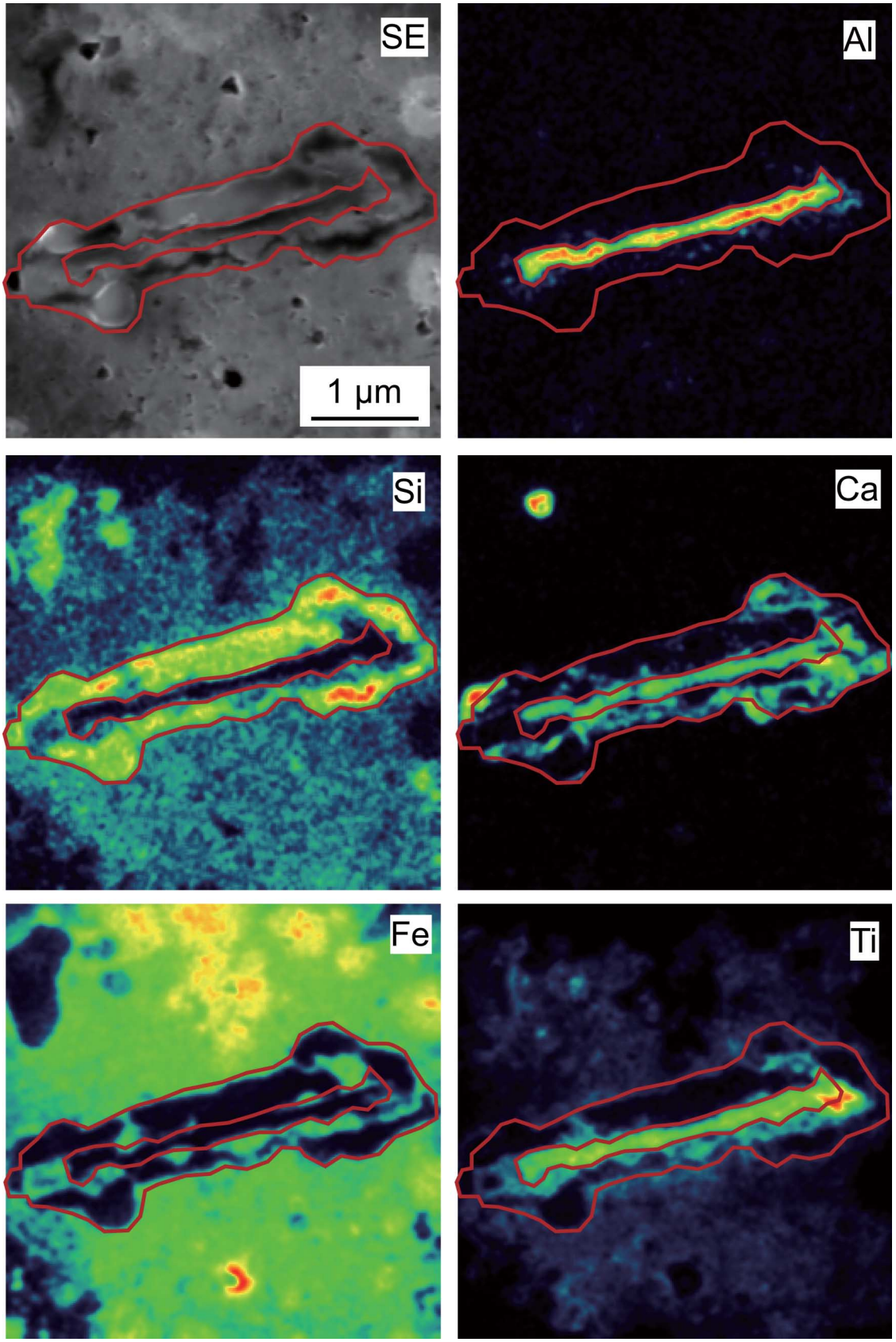

Fig. 10. Secondary electron image and Auger elemental maps of a complex Group 1 grain from the Krymka LL chondrite (Leitner et al., 2014).

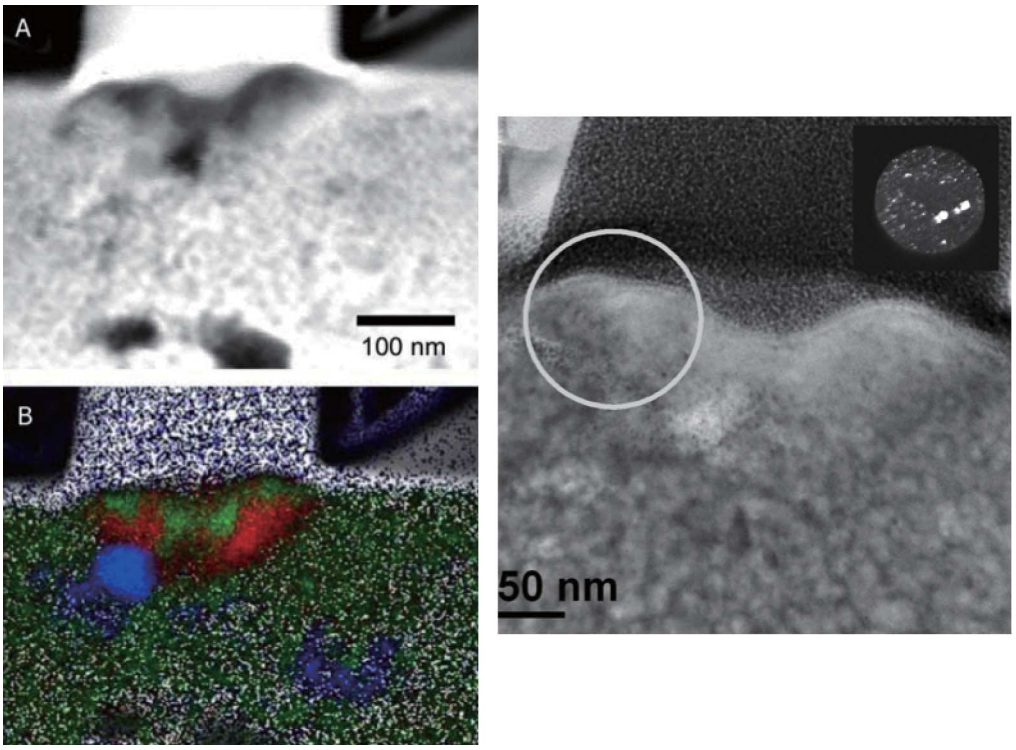

Fig. 11. Grain 4c-3 from the CR3 chondrite MET 00426. Left: (a) HAADF image and (b) principal component EDX map showing compositional heterogeneity in the grain (red: Mg-O, blue: Fe-S, green: Si-O). Right: bright-field and dark-field (inset) images. The circle indicates the SAED aperture position for the dark-field image. The SAED pattern (not shown) is consistent with an amorphous + nanocrystalline microstructure (Stroud et al., 2009).

Mineralogies and Physical Properties

The number of presolar silicate grains that have been examined by TEM is still limited (~40 grains). However, the data provided by these studies has revealed important information about the structural properties of these grains. Approximately a quarter of the grains analyzed by TEM to date are crystalline; the bulk of the rest are amorphous (~55%), with GEMS making up ~20% of these. The remainder are composite grains.

The crystalline silicates identified to date include forsteritic and fayalitic olivine (Messenger *et al*., 2003, 2005; Busemann *et al*., 2009; Vollmer *et al*., 2009b; Stojic *et al*., 2013; Stroud *et al*., 2014), enstatite and orthopyroxene (Nguyen *et al*., 2013; Vollmer *et al*., 2013; Stroud *et al*., 2014), and assemblages of polycrystalline olivine and pyroxene grains (Messenger *et al*., 2010; Nguyen *et al*., 2010b; Zega *et al*., 2014). Olivine is significantly more abundant than pyroxene, consistent with expectations from condensation calculations and experimental work (Vollmer *et al*., 2013).

The most notable crystalline silicate discovered to date is a $MgSiO_3$ grain with a high-pressure perovskite-like structure (Vollmer *et al*., 2007). The grain is likely to have formed by transformation of a silicate precursor triggered by a shock wave, although crystallization by chemical vapor deposition is also a possibility (Vollmer *et al*., 2007). Shock transformation could occur in the interstellar medium or in the direct vicinity of the parent star. The grain has an extreme Group 1 oxygen isotopic composition, which may have formed in the ejecta of an ONe or CO nova; a nova explosion would drive a strong shock front through previously condensed silicates, possibly accounting for the phase transformation (Vollmer *et al*., 2007). Enstatite is expected to be the most abundant silicate to condense in nova ejecta (José *et al*., 2004), lending additional support to this scenario.

The amorphous grains that dominate the presolar silicate inventory exhibit a variety of compositions and structural features. Some are non-stoichiometric with heterogeneous compositions (Nguyen *et al*., 2007, 2010a; Stroud *et al*., 2009, 2014; Vollmer *et al*., 2009b), but amorphous grains compositionally consistent with olivine or pyroxene are also observed (Nguyen *et al*., 2010b, 2011). In addition to compositional heterogeneity, some grains exhibit structural heterogeneity, with regions of amorphous material intimately mixed with domains of nanocrystalline material (Fig. 11), indicating crystalliza-

tion under complex non-equilibrium conditions (Stroud *et al*., 2009; Vollmer *et al*., 2013).

Composite grains have also been examined by FIB-TEM. Stroud *et al*. (2013) identified an O-rich presolar grain from the DOM 08006 CO chondrite consisting, like the grain from Krymka discussed above, of a calcium-aluminum-rich core surrounded by a silicate rim. While the core could not be indexed to a specific phase, due to the small sizes of several compositionally distinct grains, the rim consists of a polycrystalline aggregate of forsteritic olivine grains. Another composite grain, found in an IDP, consists of crystalline spinel surrounded by an amorphous non-stoichiometric rim of Mg- and Si-rich silicate (Nguyen *et al*., 2014). Composite grains composed only of silicates are also observed, such as a grain from QUE 99177 that consists of an enstatite core surrounded by an amorphous silicate rim (Nguyen *et al*., 2013). The occurrence of such composite grains indicates that the circumstellar environments around O-rich evolved stars are complex, with varying physical and chemical conditions that allow the contemporaneous formation of structurally and compositionally distinct grains.

Comparison with Astronomical Observations

Astronomical observations indicate that most circumstellar silicates are amorphous, with crystalline silicates typically making up less than 10% of stellar condensates (Tielens *et al*., 1998; Kemper *et al*., 2001). Crystalline silicates have been observed around young main sequence stars (Waelkens *et al*., 1996; Malfait *et al*., 1998) and oxygen-rich AGB stars (Waters *et al*., 1996; Demyk *et al*., 2000); in rare cases, stars with up to 75% crystalline silicates have been observed (Molster *et al*., 2001). Enstatite appears to be about 3–4 times more abundant than forsterite for most stellar sources (Molster *et al*., 2002a). Although the broad features of amorphous silicates do not allow a detailed analysis, the spectra indicate primarily olivine compositions, with pyroxene compositions probably representing less than 10% of the total amorphous silicate mass (Demyk *et al*., 2000).

Auger analyses show that the number of grains with pyroxene-like compositions is similar to the number with olivine-like compositions, in contrast to expectations from either predominantly crystalline or predominantly amorphous sources, from which one would anticipate primarily pyroxene or olivine compositions, respectively. A large fraction of presolar silicate grains also have compositions that are intermediate between those of olivine and pyroxene (Fig. 8). A study by Min *et al*. (2007) suggests that amorphous silicates in the interstellar medium are expected to have a stoichiometry in between that of olivine and pyroxene type silicates, with an O/Si ratio of 3.5, identical to the average O/Si ratio of intermediate type grains.

Among grains whose structures have been determined by TEM, the presolar silicate population shows a significantly higher abundance of olivine over pyroxene, in contrast to astronomical observations. Moreover, TEM studies indicate that some presolar silicates consist of mixtures of both amorphous and nanocrystalline material; it seems likely that such grains would exhibit broad featureless spectra similar to fully amorphous grains, suggesting that circumstellar disks could contain a larger fraction of crystalline material than previously estimated (Stroud *et al*., 2009).

The presence of SiO_2 in the presolar silicate grain population confirms observational evidence for its presence in circumstellar envelopes. Silica has tentatively been observed in the O-rich dust shells around evolved stars (Molster *et al*., 2002b), and spectra of BP Piscium, a first ascent giant star, were recently modeled by material that included crystalline sub-micrometer-sized cristobalite (Melis *et al*., 2010), a polymorph of silica. In addition, observations of several supernova remnants indicate the possible presence of silica dust (Rho *et al*., 2008, 2009), consistent with the recent identification of SiO_2 grains with a likely supernova origin (Haenecour *et al*., 2013a).

Secondary Processing

Because presolar silicates are fragile and easily affected by secondary processing, they can be used as a tool to investigate nebular and parent body processes in the early solar nebula. Abundance variations within individual meteorites have provided information about the secondary processes experienced by these materials. Fine-grained material in carbonaceous chondrites occurs either as interchondrule matrix or as rims around chondrules/CAIs. Haenecour *et al*. (2013b, 2014a) compared the abundances of presolar grains in matrix material and fine-grained chondrule rims from three CO3 chondrites, LAP 031117, DOM 08006 and ALHA77307. The abundances of O-rich presolar grains in the matrices of the three meteorites are the same, within errors, and the abundances of presolar SiC are the same in both the matrix and chondrule rims in these meteorites, consistent with an origin of these fine-grained materials in CO3 chondrites from nebular reservoirs with similar presolar grain abundances. However, the abundances of presolar silicates are significantly lower in the chondrule rims than in the matrix, suggesting destruction or re-equilibration of the oxygen isotopic compositions of some silicates in the rims. Initial FIB-TEM analysis of a matrix area and chondrule rim from LAP 031117 indicated that while the matrix area is mostly composed of anhydrous amorphous material, the rim shows the presence of phyllosilicates,

clear evidence that aqueous alteration accounts for the lower presolar silicate abundances in the chondrule rim (Haenecour *et al*., 2014b, 2015). In contrast, Leitner *et al*. (2013b) observed that presolar silicate abundances were a factor of two higher in the chondrule rims than in interchondrule matrix areas of three CR chondrites, suggesting locally distinct degrees of aqueous alteration in these meteorites.

Secondary processing can also affect the elemental compositions of presolar silicate grains. As shown in Fig. 1, the presolar silicate abundance in the ungrouped C chondrite Adelaide is a factor of two lower than in the most primitive carbonaceous chondrites. Although ungrouped, Adelaide is similar to the CO3 chondrite ALHA77307 in terms of matrix abundance, mineralogy and chondrule size (Brearley, 1991). However, although both meteorites contain amorphous material in their matrices, the matrix of Adelaide is more crystalline than that of ALHA77307, suggesting that it has experienced some thermal annealing (Brearley, 1991). The presolar silicates in Adelaide are distinctly more Fe-rich than presolar silicates from other meteorites (Fig. 8), with a median Fe concentration of ~26 at.% vs. median Fe concentrations of 12–14 at.% in other carbonaceous chondrites (Floss and Stadermann, 2012). This is also reflected in the (Fe+Mg+Ca)/Si ratios of the grains from Adelaide, the majority of which have ratios significantly higher than that of olivine (Fig. 7). Thermal metamorphism can increase the Fe contents of originally Mg-rich grains (Jones and Rubie, 1991), and annealing of Adelaide matrix material is likely responsible both for the elevated Fe contents in its presolar silicates, with Fe permeating into the grains from the surrounding Fe-rich matrix, and for its lower presolar silicate abundances (Floss and Stadermann, 2012). FIB/TEM analysis of one presolar spinel from Adelaide exhibits local enrichment of Fe in a ~50 nm band along the border of the grain (Zega and Floss, 2013), providing additional confirmation of this process.

Secondary processing has also affected the Fe abundances of presolar silicates in MIL 07687 (Floss and Brearley, 2014, 2015), another ungrouped meteorite with affinities to the CO chondrites. The most unusual feature of this meteorite is that it appears to have undergone a unique style of highly localized aqueous alteration, in which primitive Fe-poor matrix areas are intimately intermingled with extensively altered Fe-rich matrix areas (Brearley, 2012, 2013). Moreover, rather than phyllosilicates, the altered regions are dominated by fibrous Fe oxyhydroxides, suggesting alteration under highly oxidizing conditions. In contrast to the observations for Adelaide, presolar silicates in the altered regions of MIL 07687 have lower median Fe contents than those in the unaltered areas, suggesting loss of Fe through leaching from the grains during aqueous alteration and subsequent formation of Fe oxyhydroxides. Presolar grain abundances are higher in the unaltered Fe-poor areas than in the altered regions, but the difference is larger for SiC than it is for presolar silicates, in contrast to expectations. The fact that alteration in MIL 07687 took place under highly oxidizing conditions may account for the enhanced susceptibility of SiC to partial destruction in this meteorite (Floss and Brearley, 2015).

Conclusions and Outlook

The past ten years has provided a wealth of information about the abundances, isotopic and elemental compositions, and mineralogies of presolar silicate grains. Oxygen isotopic compositions of presolar silicates indicate that the majority of these grains form in low-mass red giant or AGB stars of close-to-solar metallicity. However, the isotopic compositions of some O-rich presolar grains are not consistent with stellar evolution models, indicating that our understanding of the origins of these grains and the nucleosynthetic processes involved is still incomplete.

Presolar silicates are more abundant and more diverse in mineralogy and elemental composition than most other phases in the presolar grain inventory, providing important information about the stellar environments in which they condensed. The majority of these grains are ferromagnesian silicates, similar to olivine and pyroxene, or have compositions intermediate between these phases. The high Fe concentrations of many presolar silicates reflect formation under kinetic conditions, consistent with models of silicate dust formation in thermally pulsing AGB stars. Many presolar silicates are also amorphous with heterogeneous compositions, further evidence of their formation under non-equilibrium conditions.

Because presolar silicates are highly susceptible to alteration, they can also provide information about conditions in the nebular and/or parent body environments that they have experienced. Abundance variations are correlated with the degree of secondary processing experienced by the meteorite parent bodies, and elemental as well as isotopic changes due to thermal processing and/or aqueous alteration have been observed in the presolar silicates from some meteorites. Variations have also been noted in the relative proportions of the O isotopic grain groups, and may reflect spatial and/or temporal differences in the incorporation of stardust into the extraterrestrial materials in which they are found.

Presolar silicate grains complement studies of other presolar grain types and provide unique information about stellar evolution and nucleosynthetic processes. The studies carried out on these grains to date have shown that analyses of multiple isotopic systems are needed to understand the origins of the grains, as well as the

nucleosynthetic processes taking place in their parent stars. This is particularly true for rare grains, such as rare extreme Group 1 silicates, whose origins are still debated. Additional TEM work is also needed to fully characterize the diversity of grains in the inventory of O-rich presolar grains, which will help inform astronomical observations of the circumstellar envelopes around stellar objects.

Acknowledgments—We thank A. N. Nguyen and L. R. Nittler for constructive reviews, which significantly improved this paper. This work was supported by NASA grant NNX14AG25G to C.F. and NASA Earth and Space Sciences Fellowship NNX12AN77H to P.H.

References

Abreu, N. M. and Brearley, A. J. (2010) Early solar system processes recorded in the matrices of two highly pristine CR3 carbonaceous chondrites, MET 00426 and QUE 99177. *Geochim. Cosmochim. Acta* **74**, 1146–1171.

Alexander, C. M. O'D., Nittler, L. R. and Tera, F. (2001) The search for presolar silicates and the ^{54}Cr carrier. *Lunar Planet. Sci. XXXII*, #2191.

Amari, S., Anders, E., Virag, A. and Zinner, E. (1990) Interstellar graphite in meteorites. *Nature* **345**, 238–240.

Amari, S., Lewis, R. S. and Anders, E. (1994) Interstellar grains in meteorites: I. Isolation of SiC, graphite, and diamond; size distributions of SiC and graphite. *Geochim. Cosmochim. Acta* **58**, 459–470.

Anders, E. and Zinner, E. (1993) Interstellar grains in primitive meteorites: diamond, silicon carbide, and graphite. *Meteoritics* **28**, 490–514.

Bernatowicz, T., Fraundorf, G., Ming, T., Anders, E., Wopenka, B., Zinner, E. and Fraundorf, P. (1987) Evidence for interstellar SiC in the Murray carbonaceous meteorite. *Nature* **330**, 728–730.

Bernatowicz, T., Cowsik, R., Gibbons, P. C., Lodders, K., Fegley, B., Amari, S. and Lewis, R. S. (1996) Constraints on stellar grain formation from presolar graphite in the Murchison meteorite. *Astrophys. J.* **472**, 760–782.

Black, D. C. (1972) On the origins of trapped helium, neon and argon isotopic variations in meteorites II. Carbonaceous meteorites. *Geochim. Cosmochim. Acta* **36**, 377–394.

Black, D. C. and Pepin, R. O. (1969) Trapped neon in meteorites. II. *Earth Planet. Sci. Lett.* **6**, 395–405.

Bland, P. A., Stadermann, F. J., Floss, C., Rost, D., Vicenzi, E. P., Kearsley, A. T. and Benedix, G. K. (2007) A cornucopia of presolar and early solar system materials at the micrometer size range in primitive chondrite matrix. *Meteorit. Planet. Sci.* **42**, 1417–1427.

Boato, G. (1954) The isotopic composition of hydrogen and carbon in the carbonaceous chondrites. *Geochim. Cosmochim. Acta* **6**, 209–220.

Boothroyd, A. I. and Sackman, I. J. (1999) The CNO isotopes: deep circulation in red giants and first and second dredge-up. *Astrophys. J.* **510**, 232–250.

Bose, M., Zhao, X., Floss, C., Stadermann, F. J. and Lin, Y. (2010a) Stardust material in the paired enstatite meteorites: SAH 97096 and SAH 97159. *Proc. Int'l Symp. "Nuclei in the Cosmos—XI"*, Proc. Sci. (NIC-XI), 138.

Bose, M., Floss, C. and Stadermann, F. J. (2010b) An investigation into the origin of Fe-rich presolar silicates in Acfer 094. *Astrophys. J.* **714**, 1624–1636.

Bose, M., Floss, C., Stadermann, F. J., Stroud, R. M. and Speck, A. K. (2012) Stellar and interstellar material in the CO3 chondrite ALHA77307: an isotopic and elemental investigation. *Geochim. Cosmochim. Acta* **93**, 77–101.

Bose, M., Zega, T. J. and Williams, P. (2014) Assessment of alteration processes on circumstellar and interstellar grains in Queen Alexandra Range 97416. *Earth Planet. Sci. Lett.* **399**, 128–138.

Bradley, J. P. (1994a) Nanometer-scale mineralogy and petrography of fine-grained aggregates in anhydrous interplanetary dust particles. *Geochim. Cosmochim. Acta* **58**, 2123–2134.

Bradley, J. P. (1994b) Chemically anomalous preaccretionally irradiated grains in interplanetary dust particles from comets. *Science* **265**, 925–929.

Bradley, J. P. (2013) Comment—How and where did GEMS form? *Geochim. Cosmochim. Acta* **107**, 336–340.

Bradley, J. P. and Dai, Z. R. (2004) Mechanism of formation of glass with embedded metal and sulfides. *Astrophys. J.* **617**, 650–655.

Brearley, A. J. (1991) Mineralogical and chemical studies of matrix in the Adelaide meteorite, a unique carbonaceous chondrite with affinities to ALH 77307 (CO3). *Lunar Planet. Sci. XXII*, 133–134.

Brearley, A. J. (1993) Matrix and fine-grained rims in the unequilibrated CO3 chondrite, ALHA77307: origins and evidence for diverse, primitive nebular dust components. *Geochim. Cosmochim. Acta* **57**, 1521–1550.

Brearley, A. J. (2012) MIL 07687—an intriguing, very low petrologic type 3 carbonaceous chondrite with a unique style of aqueous alteration. *Lunar Planet. Sci. XLIII*, #1233.

Brearley, A. J. (2013) Miller Range MIL 07687: a unique carbonaceous chondrite with a complex record of partial aqueous alteration. *Meteorit. Planet. Sci.* **47**, #5206.

Busemann, H., Nguyen, A. N., Cody, G. D., Hoppe, P., Kilcoyne, A. L. D., Stroud, R. M., Zega, T. J. and Nittler, L. R. (2009) Ultra-primitive interplanetary dust particles from the comet 26P/Grigg-Skjellerup dust stream collection. *Earth Planet. Sci. Lett.* **288**, 44–57

Carrez, P., Demyk, K., Cordier, P., Gengembre, L., Grimblot, J., d'Hendecourt, L., Jones, A. P. and Leroux, H. (2002) Low-energy helium ion irradiation-induced amorphization and chemical changes in olivine: insights for silicate dust evolution in the interstellar medium. *Meteorit. Planet. Sci.* **37**, 1599–1614.

Choi, B.-G., Huss, G. R., Wasserburg, G. J. and Gallino, R. (1998) Presolar corundum and spinel in ordinary chondrites: origins from AGB stars and a supernova. *Science* **282**, 1284.

Choi, B.-G., Wasserburg, G. J. and Huss, G. R. (1999) Circumstellar hibonite and corundum and nucleosynthesis in asymptotic giant branch stars. *Astrophys. J.* **522**, L133–L136.

Cristallo, S., Piersanti, L., Straniero, O., Gallino, R.,

Dominguez, I., Abia, C., Di Rico, G., Quintini, M. and Bisterzo, S. (2011) Evolution, nucleosynthesis, and yields of low-mass asymptotic giant branch stars at different metallicities. II. The FRUITY database. *Astrophys. J.* **197**, doi:10.1088/0067-0049/197/2/17.

Croat, T. K., Bernatowicz, T., Amari, S., Messenger, S. and Stadermann, F. J. (2003) Structural, chemical, and isotopic microanalytical investigations of graphite from supernovae. *Geochim. Cosmochim. Acta* **67**, 4705–4725.

Croat, T. K., Stadermann, F. J. and Bernatowicz, T. J. (2005) Presolar graphite from AGB stars: microstructure and s-process enrichment. *Astrophys. J.* **631**, 976–987.

Davidson, J., Nittler, L. R., Alexander, C. M. O'D. and Stroud, R. M. (2014) Presolar materials and nitrogen isotopic anomalies in the unique carbonaceous chondrite Miller Range 07687. *Lunar Planet. Sci. XLV*, #1376.

Davidson, J., Schrader, D. L., Alexander, C. M. O'D., Lauretta, D. S., Busemann, H., Franchi, I. A., Greenwood, R. C., Connolly, H. C., Domanik, K. J. and Verchovsky, A. (2015) Petrography, stable isotope compositions, microRaman spectroscopy and presolar components of Roberts Massif 04133: a reduced CV3 carbonaceous chondrite. *Meteorit. Planet. Sci*. **49**, 2133–2151.

Demyk, K., Dartois, E., Wiesemeyer, H., Jones, A. P. and d'Hendecourt, L. (2000) Structure and chemical composition of the silicate dust around OH/IR stars. *Astron. Astrophys*. **364**, 170–178.

Demyk, K., Carrez, Ph., Leroux, H., Cordier, P., Jones, A. P., Borg, J., Quirico, E., Raynal, P. I. and d'Hendecourt, L. (2001) Structural and chemical alteration of crystalline olivine under low energy He^+ irradiation. *Astron. Astrophys*. **368**, L38–L41.

Dobrica, E., Engrand, C., Leroux, H., Rouzaud, J.-N. and Duprat, J. (2012) Transmission electron microscopy of CONCORDIA ultracarbonaceous Antarctic micrometeorites (UCAMMs): mineralogical properties. *Geochim. Cosmochim. Acta* **76**, 68–82.

Ebata, S., Nagashima, K., Itoh, S., Kobayashi, S., Sakamoto, N., Fagan, T. J. and Yurimoto, H. (2006) Presolar silicate grains in enstatite chondrites. *Lunar Planet. Sci. XXXVII*, #1619.

Ferrarotti, A. S. and Gail, H.-P. (2001) Mineral formation in stellar winds II. Effects of Mg/Si abundance variations on dust composition in AGB stars. *Astron. Astrophys*. **371**, 133–151.

Floss, C. and Brearley, A. J. (2014) Presolar grain abundance variations in the unique carbonaceous chondrite MIL 07687. *Meteorit. Planet. Sci*. **49**, #5183.

Floss, C. and Brearley, A. J. (2015) Effects of secondary processing on presolar grain abundances and compositions in the unique carbonaceous chondrite Miller Range 07687. *Lunar Planet. Sci. XLVI*, #1004.

Floss, C. and Stadermann, F. J. (2009) Auger Nanoprobe analysis of presolar ferromagnesian silicate grains from primitive CR chondrites QUE 99177 and MET 00426. *Geochim. Cosmochim. Acta* **73**, 2415–2440.

Floss, C. and Stadermann, F. J. (2012) Presolar silicate and oxide abundances and compositions in the ungrouped carbonaceous chondrite Adelaide and the K chondrite Kakangari: the effects of secondary processing. *Meteorit. Planet. Sci*. **47**, 1869–1883.

Floss, C., Stadermann, F. J., Bradley, J. P., Dai, Z. R., Bajt, S., Graham, G. and Lea, A. S. (2006) Identification of isotopically primitive interplanetary dust particles: a NanoSIMS isotopic imaging study. *Geochim. Cosmochim. Acta* **70**, 2371–2399.

Floss, C., Stadermann, F. J., Mertz, A. F. and Bernatowicz, T. J. (2010) A NanoSIMS and Auger Nanoprobe investigation of an isotopically primitive interplanetary dust particle from the 55P/Tempel-Tuttle targeted stratospheric dust collector. *Meteorit. Planet. Sci*. **45**, 1889–1905.

Floss, C., Noguchi, T. and Yada, T. (2012) Ultracarbonaceous Antarctic micrometeorites: origins and relationships to primitive extraterrestrial materials. *Lunar Planet. Sci. XLIII*, #1217.

Floss, C., Stadermann, F. J., Kearsley, A. T., Burchell, M. J. and Ong, W. J. (2013) The abundance of presolar grains in comet 81P/Wild 2. *Astrophys. J*. **763**, doi:10.1088/0004-637X/763/2/140.

Floss, C., Le Guillou, C. and Brearley, A. (2014) Coordinated NanoSIMS and FIB-TEM analyses of organic matter and associated matrix materials in CR3 chondrites. *Geochim. Cosmochim. Acta* **139**, 1–25.

Floss, C., Wiesman, H. and Haenecour, P. (2015) NanoSIMS and Auger analysis of impact craters from the Genesis 'aluminum kidney'. *Meteorit. Planet. Sci*. **50**, #5010.

Gail, H.-P. and Sedlmayr, E. (1999) Mineral formation in stellar winds I. Condensation sequence of silicate and iron grains in stationary oxygen rich outflows. *Astron. Astrophys*. **347**, 594–616.

Gail, H.-P., Zhukovska, S. V., Hoppe, P. and Trieloff, M. (2009) Stardust from asymptotic giant branch stars. *Astrophys. J*. **698**, 1136–1154.

Goldstein, J. I., Newbury, D. E., Echlin, P., Joy, D. C., Romig, A. D., Lyman, C. E., Fiori, C. and Lifshin, E. (1992) *Scanning Electron Microscopy and X-ray Microanalysis*. Plenum Press.

Graham, G. A., Teslich, N. E., Kearsley, A. T., Stadermann, F. J., Stroud, R. M., Dai, Z., Ishii, H. A., Hutcheon, I. A., Bajt, S., Snead, C. J., Weber, P. K. and Bradley, J. P. (2008) Applied focused ion beam techniques for sample preparation of astromaterials for integrated nanoanalysis. *Meteorit. Planet. Sci*. **43**, 561–569.

Greshake, A. (1997) The primitive matrix components of the unique carbonaceous chondrite Acfer 094: a TEM study. *Geochim. Cosmochim. Acta* **61**, 437–452.

Gyngard, F., Nittler, L. R., Zinner, E. and José, J. (2010a) Oxygen-rich stardust grains from novae. *Proc. Int'l Symp. "Nuclei in the Cosmos—XI"*, Proc. Sci. (NIC-XI), 141.

Gyngard, F., Zinner, E., Nittler, L., Morgand, A., Stadermann, F. J. and Hynes, K. M. (2010b) Automated NanoSIMS measurements of spinel stardust from the Murray meteorite. *Astrophys. J*. **717**, 107–120.

Gyngard, F., Nittler, L. R., Zinner, E., José, J. and Cristallo, S. (2011) New reaction rates and implications for nova nucleosynthesis and presolar grains. *Lunar Planet. Sci. XLII*, #2675.

Haenecour, P. and Floss, C. (2011) High abundance of stardust

in the CO3.0 chondrite LaPaz 031117. *Meteorit. Planet. Sci*. **46**, A85.

Haenecour, P. and Floss, C. (2012) Stardust in fine-grained chondrule rims and matrix in LaPaz 031117: insights into the conditions of dust accretion in the solar nebula. *Lunar Planet. Sci. XLIII*, #1107.

Haenecour, P., Floss, C. and Yada, T. (2012) Heterogeneous distribution of supernova silicate and oxide grains in the solar system? *Meteorit. Planet. Sci*. **47**, #5220.

Haenecour, P., Zhao, X., Floss, C., Lin, Y. and Zinner, E. (2013a) First observation of silica grains from core collapse supernovae. *Astrophys. J. Lett*. **768**, doi:10.1088/2041-8205/768/1/L17.

Haenecour, P., Floss, C., Jolliff, B. L. and Carpenter, P. (2013b) Presolar grains in fine-grained chondrule rims: re-equilibration of oxygen isotopic compositions in some presolar silicates by heating. *Lunar Planet. Sci. XLIV*, #1150.

Haenecour, P., Floss, C., Jolliff, B. L., Zega, T. J., Bose, M. and Carpenter, P. (2014a) Presolar silicates as tracers of the formation of fine-grained chondrule rims in CO3 chondrites. *Lunar Planet. Sci. XLV*, #1316.

Haenecour, P., Floss, C. and Zega T. J. (2014b) Spatial variation of presolar silicate abundances in CO3 chondrites: correlation with aqueous alteration? *Meteorit. Planet. Sci*. **49**, #5042.

Haenecour, P., Floss, C., Zega, T. J., Croat, T. K. and Jolliff, B. L. (2015) Presolar silicates as evidence of sporadic aqueous alteration in primitive CO3 chondrites. *Lunar Planet. Sci. XLVI*, #1160.

Halbout, J., Mayeda, T. K. and Clayton, R. N. (1986) Carbon isotopes and light element abundances in carbonaceous chondrites. *Earth Planet. Sci. Lett*. **80**, 1–18.

Henning, T. (2009) Cosmic silicate dust. *EAS Publication Series* **35**, pp. 103–114.

Henning, T. (2010) Cosmic silicates. *Ann. Rev. Astron. Astrophys*. **48**, 21–46.

Huss, G. R., Fahey, A. J., Gallino, R. and Wasserburg, G. J. (1994) Oxygen isotopes in circumstellar Al_2O_3 grains from meteorites and stellar nucleosynthesis. *Astrophys. J*. **430**, L81–L84.

Huss, G. R., Meyer, B. S., Srinivasan, G., Goswami, J. N. and Sahijpal, S. (2009) Stellar sources of the short-lived radionuclides in the early solar system. *Geochim. Cosmochim. Acta* **73**, 4922–4945.

Hynes, K. M. and Gyngard, F. (2009) The presolar grain database: http://presolar.wustl.edu/~pgd. *Lunar Planet Sci. XL*, #1198.

Ishii, H. A., Bradley, J. P., Dai, Z. R., Chi, M., Kearsley, A. T., Burchell, M. J., Browning, N. D. and Molster, F. (2008) Comparison of Comet 81P/Wild 2 dust with interplanetary dust from comets. *Science* **318**, 447–450.

Jones, R. H. and Rubie, D. C. (1991) Thermal histories of CO3 chondrites: application of olivine diffusion modeling to parent body metamorphism. *Earth Planet. Sci. Lett*. **106**, 73–86.

José, J., Hernanz, M., Amari, S., Lodders, K. and Zinner, E. (2004) The imprint of nova nucleosynthesis in presolar grains. *Astrophys. J*. **612**, 414–428.

Karakas, A. I. and Lattanzio, J. C. (2014) The Dawes review 2: nucleosynthesis and stellar yields of low and intermediate-mass stars. *Pub. Astron. Soc. Austr*. **31**, doi:10.1017/pasa.2014.21.

Keller, L. P. and Messenger, S. (2011) On the origins of GEMS grains. *Geochim. Cosmochim. Acta* **75**, 5336–5365.

Keller, L. P. and Messenger, S. (2013) On the origin of GEMS grains: a reply. *Geochim. Cosmochim. Acta* **107**, 341–344.

Kemper, F., Waters, L. B. F. M., de Koter, A. and Tielens, A. G. G. M. (2001) Crystallinity versus mass-loss rate in asymptotic giant branch stars. *Astron. Astrophys*. **369**, 132–141.

Kobayashi, S., Tonotani, A., Sakamoto, N., Nagashima, K., Krot, A. N. and Yurimoto, H. (2005) Presolar silicate grains from primitive carbonaceous chondrites Y-81025, ALHA77307, Adelaide and Acfer 094. *Lunar Planet. Sci. XXXVI*, #1931.

Kodolányi, J. and Hoppe, P. (2011a) Magnesium isotope measurements on presolar silicate grains from AGB stars. *Lunar Planet. Sci. XLII*, #1094.

Kodolányi, J. and Hoppe, P. (2011b) The Mg isotope composition of presolar silicate grains from AGB stars: constraints on the Mg isotope inventory of the local interstellar medium at solar birth. *Meteorit. Planet. Sci*. **46**, #5255.

Kodolányi, J., Hoppe, P., Gröner, E., Pauly, C. and Mücklich, F. (2014) The Mg isotope composition of presolar silicate grains from red giant stars. *Geochim. Cosmochim. Acta* **140**, 577–605.

Lee, T. (1988) Implications of isotopic anomalies for nucleosynthesis. *Meteorites and the Early Solar System* (Kerridge, J. F. and Matthews M. S., eds.), 1063–1089, University of Arizona Press, Tucson.

Leitner, J., Hoppe, P. and Heck, P. R. (2010) First discovery of presolar material of possible supernova origin in impact residues from comet 81P/Wild 2. *Lunar Planet. Sci. XLI*, #1607.

Leitner, J., Hoppe, P. and Zipfel, J. (2011) The stardust inventory of CR chondrite GRA 95229 and GRA 06100 assessed by NanoSIMS. *Lunar Planet. Sci. XLII*, #1713.

Leitner, J., Vollmer, C., Hoppe, P. and Zipfel, J. (2012a) Characterization of presolar material in the CR chondrite Northwest Africa 852. *Astrophys. J*. **745**, doi:10.1088/0004-637X/745/1/38.

Leitner, J., Heck, P. R., Hoppe, P. and Huth, J. (2012b) The C-, N-, and O-isotopic composition of cometary dust from comet 81P/Wild 2. *Lunar Planet. Sci. XLIII*, #1839.

Leitner, J., Kodolányi, J., Hoppe, P. and Floss, C. (2012c) Laboratory analysis of presolar silicate stardust from a nova. *Astrophys. J. Lett*. **754**, doi:10.1088/2041-8205/754/2/L41.

Leitner, J., Vollmer, C., Hoppe, P. and Zipfel, J. (2012d) Abundant primitive phases in fine-grained chondrule rims of CR and related chondrites. *Meteorit. Planet. Sci*. **47**, #5191.

Leitner, J., Hoppe, P. and Zipfel, J. (2012e) The stardust inventories of Graves Nunataks 95229 and Renazzo: implications for the distribution of presolar grains in CR chondrites. *Lunar Planet. Sci. XLIII*, #1835.

Leitner, J., Metzler, K., Vollmer, C. and Hoppe, P. (2013a) Search for presolar grains in fine-grained rims: first results from CM chondrites and Acfer 094. *Lunar Planet. Sci. XLIV*, #2273.

Leitner, J., Vollmer, C., Hoppe, P. and Zipfel, J. (2013b) Char-

acterization of presolar material in fine-grained chondrule rims and matrix of CR chondrites. *Meteorit. Planet. Sci*. **48**, #5175.

Leitner, J., Metzler, K. and Hoppe, P. (2014) Characterization of presolar grains in cluster chondrite clasts from unequilibrated ordinary chondrites. *Lunar Planet Sci. XLV*, #1099.

Lewis, R. S., Tang, M., Wacker, J. F., Anders, E. and Steel, E. (1987) Interstellar diamonds in meteorites. *Nature* **326**, 160–162.

Lodders, K. and Fegley, B. (1999) Condensation chemistry of circumstellar grains. *Asymptotic Giant Branch Stars* (Le Bertre, T., Lebre, A. and Waelkens, C., eds.), 279–289, Astronomical Society of the Pacific, San Francisco.

Malfait, K., Waelkens, C., Waters, L. B. F. M., Vandenbussche, B., Huygen, E. and de Graauw, M. S. (1998) The spectrum of the young star HD 100546 observed with the Infrared Space Observatory. *Astron. Astrophys*. **332**, L25–L28.

Marhas, K. K., Hoppe, P., Stadermann, F. J., Floss, C. and Lea, A. S. (2006) The distribution of presolar grains in CI and CO meteorites. *Lunar Planet. Sci. XXXVII*, #1959.

Marhas, K. K., Amari, S., Gyngard, F., Zinner, E. and Gallino, R. (2008) Iron and nickel isotopic ratios in presolar SiC grains. *Astrophys. J*. **689**, 622–645.

McKeegan, K. D., Aléon, J., Bradley, J., Brownlee, D. E., Busemann, H., Butterworth, A., Chaussidon, M., Fallon, S., Floss, C., Gilmour, J., Gounelle, M., Graham, G., Guan, Y., Heck, P. R., Hoppe, P., Hutcheon, I. D., Huth, J., Ishii, H., Ito, M., Jacobsen, S. B., Kearsley, A., Leshin, L. A., Liu, M.-C., Lyon, I., Marhas, K., Marty, B., Matrajt, G., Meibom, A., Messenger, S., Mostefaoui, S., Mukhopadhyay, S., Nakamura-Messenger, K., Nittler, L., Palma, R., Pepin, R. O., Papanastassiou, D. A., Robert, F., Schlutter, D., Snead, C. J., Stadermann, F. J., Stroud, R., Tsou, P., Westphal, A., Young, E. D., Ziegler, K., Zimmerman, L. and Zinner, E. (2006) Isotopic compositions of cometary matter returned by Stardust. *Science* **314**, 1724–1728.

Melis, C., Gielen, C., Chen, C. H., Rhee, J. H., Song, I. and Zuckerman, B. (2010) Shocks and a giant planet in the disk orbiting BP Piscium? *Astrophys. J*. **724**, 470–479.

Messenger, S. and Bernatowicz, T. (2000) Search for presolar silicates in Acfer 094. *Meteorit. Planet. Sci*. **35**, A109.

Messenger, S., Keller, L. P., Stadermann, F. J., Walker, R. M. and Zinner, E. (2003) Samples of stars beyond the solar system: silicate grains in interplanetary dust. *Science* **300**, 105–108.

Messenger, S., Keller, L. P. and Lauretta, D. S. (2005) Supernova olivine from cometary dust. *Science* **309**, 737–741.

Messenger, S., Keller, L. P., Nakamura-Messenger, K. and Nguyen, A. (2010) History of nebular processing traced by silicate stardust in IDPs. *Lunar Planet. Sci. XLI*, #2493.

Min, M., Waters, L. B. F. M., de Koter, A., Hovenier, J. W., Keller, L. P. and Markwick-Kemper, F. (2007) The shape and composition of interstellar silicate grains. *Astron. Astrophys*. **462**, 667–676.

Molster, F. J., Yamamura, I., Waters, L. B. F. M., Nyman, L.-A., Käufl, H.-U., de Jong, T. and Loup, C. (2001) IRAS 09425-6040: a carbon star surrounded by highly crystalline silicate dust. *Astron. Astrophys*. **366**, 923–929.

Molster, F. J., Waters, L. B. F. M., Tielens, A. G. G. M., Koike, C. and Chihara, H. (2002a) Crystalline silicate dust around evolved stars III. A correlation study of crystalline silicate features. *Astron. Astrophys*. **382**, 241–255.

Molster, F. J., Waters, L. B. F. M. and Tielens, A. G. G. M. (2002b) Crystalline silicate dust around evolved stars. II: The crystalline silicate complexes. *Astron. Astrophys*. **382**, 222–240.

Mostefaoui, S. (2011) The search for presolar oxides in Paris. *Meteorit. Planet. Sci*. **47**, #5170.

Mostefaoui, S. and Hoppe, P. (2004) Discovery of abundant in situ silicate and spinel grains from red giant stars in a primitive meteorite. *Astrophys. J*. **613**, L149–L152.

Nagashima, K., Krot, A. N. and Yurimoto, H. (2004) Stardust silicates from primitive meteorites. *Nature* **428**, 921–924.

Nagashima, K., Sakamoto, N. and Yurimoto, H. (2005) Destruction of presolar silicates by aqueous alteration observed in Murchison CM2 chondrite. *Lunar Planet. Sci. XXXVI*, #1671.

Nguyen, A. N. (2005) Characterization of presolar silicate grains in primitive meteorites by multi-detection raster ion imaging in the NanoSIMS. Ph.D. Thesis, Washington University, 202 pp.

Nguyen, A. N. and Messenger, S. (2014) Resolving the stellar sources of isotopically rare presolar silicate grains through Mg and Fe isotopic analyses. *Astrophys. J*. **784**, doi:10.1088/0004-1637X/1784/1082/1149.

Nguyen, A. N. and Zinner, E. (2004) Discovery of ancient silicate stardust in a meteorite. *Science* **303**, 1496–1499.

Nguyen, A. N., Zinner, E. and Lewis, R. S. (2003) Identification of presolar spinel grains from a Murray residue by multi-detection raster imaging. *Lunar Planet. Sci. XXXIV*, #1637.

Nguyen, A. N., Stadermann, F. J., Zinner, E., Stroud, R. M., Alexander, C. M. O'D. and Nittler, L. R. (2007) Characterization of presolar silicate and oxide grains in primitive carbonaceous chondrites. *Astrophys. J*. **656**, 1223–1240.

Nguyen, A. N., Nittler, L. R., Stadermann, F. J., Stroud, R. M. and Alexander, C. M. O'D. (2010a) Coordinated analyses of presolar grains in the Allan Hills 77307 and Queen Elizabeth Range 99177 meteorites. *Astrophys. J*. **719**, 166–189.

Nguyen, A. N., Keller, L. P., Rahman, Z. and Messenger, S. (2010b) Microstructure of a supernova silicate grain. *Meteorit. Planet. Sci*. **46**, #5423.

Nguyen, A. N., Keller, L. P., Rahman, Z. and Messenger, S. (2011) Microstructure of rare silicate stardust from novae and supernovae. *Meteorit. Planet. Sci*. **47**, #5449.

Nguyen, A. N., Keller, L. P., Rahman, Z. and Messenger, S. (2012) Mineralogical studies of a highly ^{17}O-depleted and a ^{17}O-rich presolar grain from the Acfer 094 meteorite. *Lunar Planet. Sci. XLIII*, #2755.

Nguyen, A. N., Keller, L. P., Rahman, Z. and Messenger, S. (2013) Crystal structure and chemical composition of a presolar silicate from the Queen Elizabeth Range 99177 meteorite. *Lunar Planet. Sci. XLIV*, #2853.

Nguyen, A. N., Nakamura-Messenger, K., Messenger, S., Keller, L. P. and Klöck, W. (2014) Identification of a compound spinel and silicate presolar grain in a chondritic interplanetary dust particle. *Lunar Planet. Sci. XLV*, #2351.

Nguyen, A. N., Nakamura-Messenger, K., Messenger, S., Keller, L. P. and Klöck, W. (2015) Assemblage of presolar materials and early solar system condensates in chondritic porous interplanetary dust particles. *Lunar Planet. Sci. XLVI*, #2868.

Nittler, L. R. (1996) Quantitative isotopic ratio ion imaging and its application to studies of preserved stardust in meteorites. Ph.D. Thesis, Washington University, 210 pp.

Nittler, L. R. (2007) Presolar grain evidence for low-mass supernova injection into the solar nebula. *Workshop on the Chronology of Meteorites and the Early Solar System*, 125–126.

Nittler, L. R. and Hoppe, P. (2005) Are presolar silicon carbide grains from novae actually from supernovae? *Astrophys. J.* **631**, L89–L92.

Nittler, L. R., Alexander, C. M. O'D., Gao, X., Walker, R. M. and Zinner, E. K. (1994) Interstellar oxide grains from the Tieschitz ordinary chondrite. *Nature* **370**, 443–446.

Nittler, L. R., Alexander, C. M. O'D., Gao, X., Walker, R. M. and Zinner, E. (1997) Stellar sapphires: the properties and origins of presolar Al_2O_3 in meteorites. *Astrophys. J.* **483**, 475–495.

Nittler, L. R., Alexander, C. M. O'D., Wang, J. and Gao, X. (1998) Meteoritic oxide grain from supernova found. *Nature* **393**, 222.

Nittler, L. R., Alexander, C. M. O'D., Gallino. R., Hoppe, P., Nguyen, A. N., Stadermann, F. J. and Zinner, E. K. (2008) Aluminum-, calcium- and titanium-rich oxide stardust in ordinary chondrite meteorites. *Astrophys. J.* **682**, 1450–1478.

Nittler, L. R., Alexander, C. M. O'D. and Stroud, R. M. (2013) High abundance of presolar materials in CO3 chondrite Dominion Range 08006. *Lunar Planet. Sci. XLIV*, #2367.

Noguchi, T., Ohashi, N., Nishida, S., Nakamura, T., Aoki, T., Toh, S., Stephan, T. and Iwata, N. (2008) Discovery of Antarctic micrometeorites containing GEMS and enstatite whiskers. *Meteorit. Planet. Sci.* **43**, A117.

Nollett, K. M., Busso, M. and Wasserburg, G. J. (2003) Cool bottom processes on the thermally pulsing asymptotic giant branch and the isotopic composition of circumstellar dust grains. *Astrophys. J.* **582**, 1036–1058.

Ong, W. J. and Floss, C. (2013) Fe isotope nucleosynthesis: constraints from Fe isotopic analyses of presolar silicate grains from Acfer 094. *Lunar Planet. Sci. XLIV*, #1163.

Ong, W. J. and Floss, C. (2015) Iron isotopic measurements in presolar silicate and oxide grains from the Acfer 094 ungrouped carbonaceous chondrite. *Meteorit. Planet. Sci.* **50**, 1392–1407.

Ong, W. J., Floss, C. and Gyngard, F. (2012) Negative secondary ion measurements of $^{54}Fe/^{56}Fe$ and $^{57}Fe/^{56}Fe$ in presolar silicate grains from Acfer 094. *Lunar Planet. Sci. XLIII*, #1225.

Ouellette, N., Desch, S. J., Bizzarro, M., Boss, A. P., Ciesla, F. and Meyer, B. (2009) Injection mechanisms of short-lived radionuclides and their homogenization. *Geochim. Cosmochim. Acta* **73**, 4946–4962.

Ouellette, N., Desch, S. J. and Hester, J. J. (2010) Injection of supernova dust in nearby protoplanetary disks. *Astrophys. J.* **711**, 597–612.

Palmerini, S., La Cognata, M., Cristallo, S. and Busso, M. (2011) Deep mixing in evolved stars. I. The effect of reaction rate revisions from C to Al. *Astrophys. J.* **729**, doi: 10.1088/0004-637X/729/1/3.

Rauscher, T., Heger, A., Hoffman, R. D. and Woosley, S. E. (2002) Nucleosynthesis in massive stars with improved nuclear and stellar physics. *Astrophys. J.* **576**, 323–348.

Reynolds, J. H. and Turner, G. (1964) Rare gases in the chondrite Renazzo. *J. Geophys. Res.* **69**, 3263–3281.

Rho, J., Kozasa, T., Reach, W. T., Smith, J. D., Rudnick, L., DeLaney, T., Ennis, J. A., Gomez, H. and Tappe, A. (2008) Freshly formed dust in the Cassiopeia A supernova remnant as revealed by the Spitzer Space Telescope. *Astrophys. J.* **673**, 271–282.

Rho, J., Reach, W. T., Tappe, A., Hwang, U., Slavin, J., Kozasa, T. and Dunne, L. (2009) Spitzer observations of the young core-collapse supernova remnant 1E0102.2-72.3: infrared ejecta emission and dust formation. *Astronomical Society of the Pacific Conference Series* (Henning, T., Grün, E. and Steinacker, J., eds.), 22.

Rietmeijer, F. J. M., Pun, A. and Nuth, J. A. (2009) Dust formation and evolution in a Ca-Fe-SiO-H_2-O_2 vapour phase condensation experiment and astronomical implications. *Mon. Not. R. Astron. Soc.* **396**, 402–408.

Sogawa, H. and Kozasa, T. (1999) On the origin of crystalline silicate in circumstellar envelopes of oxygen-rich asymptotic giant branch stars. *Astrophys. J.* **516**, L33–L36.

Stadermann, F. J. and Bradley, J. P. (2003) The isotopic nature of GEMS in interplanetary dust particles. *Meteorit. Planet. Sci.* **38**, A123.

Stadermann, F. J., Croat, T. K., Bernatowicz, T. J., Amari, S., Messenger, S., Walker, R. M. and Zinner, E. (2005) Supernova graphite in the NanoSIMS: carbon, oxygen and titanium isotopic compositions of a spherule and its TiC subcomponents. *Geochim. Cosmochim. Acta* **69**, 177–188.

Stadermann, F. J., Hoppe, P., Floss, C., Heck, P. R., Hörz, F., Huth, J., Kearsley, A. T., Leitner, J., Marhas, K. K., McKeegan, K. D. and Stephan, T. (2008) Stardust in Stardust—the C, N, and O isotopic compositions of Wild 2 cometary matter in Al foil impacts. *Meteorit. Planet. Sci.* **43**, 299–313.

Stadermann, F. J., Floss, C., Bose, M. and Lea, A. S. (2009) The use of Auger spectroscopy for the in situ elemental characterization of sub-micrometer presolar grains. *Meteorit. Planet. Sci.* **44**, 1033–1049.

Stojic, A. N., Brenker, F. E., Leitner, J. and Hoppe, P. (2013) A coordinated in situ NanoSIMS, HR-SEM and TEM search for presolar grains in an ALHA77307 chondrule rim. *Min. Mag.* **77**, #2268.

Stroud, R. M., Floss, C. and Stadermann, F. J. (2009) Structure, elemental composition and isotopic composition of presolar silicates in MET 00426. *Lunar Planet. Sci. XL*, #1063.

Stroud, R. M., Nittler, L. R. and Alexander, C. M. O'D. (2013) Analytical electron microscopy of a CAI-like presolar grain and associated fine-grained matrix material in the Dominion Range 08006 CO3 meteorite. *Lunar Planet. Sci. XLIV*, #2315.

Stroud, R. M., De Gregorio, B. T., Nittler, L. R. and Alexander,

C. M. O'D. (2014) Comparative transmission electron microscopy studies of presolar silicate and oxide grains from the Dominion Range 08006 and Northwest Africa 5958 meteorites. *Lunar Planet. Sci. XLV*, #2806.

Tang, M. and Anders, E. (1988) Isotopic anomalies of Ne, Xe, and C in meteorites. II. Interstellar diamond and SiC: carriers of exotic noble gases. *Geochim. Cosmochim. Acta* **52**, 1235–1244.

Tielens, A. G. G. M. (1998) Interstellar depletions and the life cycle of interstellar dust. *Astrophys. J.* **499**, 267–272.

Tielens, A. G. G. M., Waters, L. B. F. M., Molster, F. J. and Justtanont, K. (1998) Circumstellar silicate mineralogy. *Astrophys. Space Sci.* **255**, 415–426.

Tonotani, A., Kobayashi, S., Nagashima, K., Sakamoto, N., Russell, S. S., Itoh, S. and Yurimoto, H. (2006) Presolar grains from primitive ordinary chondrites. *Lunar Planet. Sci. XXXVII*, #1539.

Vollmer, C. and Hoppe, P. (2010) First Fe isotopic measurement of a highly ^{17}O-enriched stardust silicate. *Lunar Planet. Sci. XLI*, #1200.

Vollmer, C., Hoppe, P., Brenker, F. E. and Holzapfel, C. (2007) Stellar $MgSiO_3$ perovskite: a shock-transformed stardust silicate found in a meteorite. *Astrophys. J.* **666**, L49–L52.

Vollmer, C., Hoppe, P. and Brenker, F. E. (2008) Si isotopic compositions of presolar silicate grains from red giant stars and supernovae. *Astrophys. J.* **684**, 611–617.

Vollmer, C., Hoppe, P., Stadermann, F. J., Floss, C. and Brenker, F. E. (2009a) NanoSIMS analysis and Auger electron spectroscopy of silicate and oxide stardust from the carbonaceous chondrite Acfer 094. *Geochim. Cosmochim. Acta* **73**, 7127–7149.

Vollmer, C., Brenker, F. E., Hoppe, P. and Stroud, R. M. (2009b) Direct laboratory analysis of silicate stardust from red giant stars. *Astrophys. J.* **700**, 774–782.

Vollmer, C., Hoppe, P. and Brenker, F. (2013) Transmission electron microscopy of Al-rich silicate stardust from asymptotic giant branch stars. *Astrophys. J.* **769**, 61.

Waelkens, C., Waters, L. B. F. M., de Graauw, M. S., Huygen, E., Malfait, K., Plets, H., Vandenbussche, B., Beintema, D. A., Boxhoorn, D. R., Habing, H. J., Heras, A. M., Kester, D. J. M., Lahuis, F., Morris, P. W., Roelfsema, P. R., Salama, A., Siebenmorgen, R., Trams, N. R., van der Bliek, N. R., Valentijn, E. A. and Wesselius, P. R. (1996) SWS observations of young main-sequence stars with dusty circumstellar disks. *Astron. Astrophys.* **315**, L245–L248.

Wasserburg, G. J., Boothroyd, A. I. and Sackmann, I. J. (1995) Deep circulation in red giant stars: a solution to the carbon and oxygen isotope puzzles? *Astrophys. J.* **447**, L37–L40.

Waters, L. B. F. M., Molster, F. J., de Jong, T., Beintema, D. A., Waelkens, C., Boogert, A. C. A., Boxhoorn, D. R., de Graauw, T., Drapatz, S., Feuchtgruber, H., Genzel, R., Helmich, F. P., Heras, A. M., Huygen, R., Izumiura, H., Justtanont, K., Kester, D. J. M., Kunze, D., Lahuis, F., Lamers, H. J. G. L. M., Leech, K. J., Loup, C., Lutz, D., Morris, P. W., Price, S. D., Roelfsema, P. R., Salama, A., Schaeidt, S. G., Tielens, A. G. G. M., Trams, N. R., Valentijn, E. A., Vandenbussche, B., van den Ancker, M. E., van Dishoeck, E. F., van Winckel, H., Wesselius, P. R. and Young, E. T. (1996) Mineralogy of oxygen-rich dust shells. *Astron. Astrophys.* **315**, L361–L364.

Watts, J. F. and Wolstenholme, J. (2003) *An Introduction to Surface Analysis by XPS and AES*. Wiley & Sons, Chichester.

Yada, T., Floss, C., Stadermann, F. J., Zinner, E., Nakamura, T., Noguchi, T. and Lea, A. S. (2008) Stardust in Antarctic micrometeorites. *Meteorit. Planet. Sci.* **43**, 1287–1298.

Yurimoto, H., Nagashima, K. and Kunihiro, T. (2003) High precision isotope micro-imaging of materials. *Appl. Surf. Sci.* **203**, 793–797.

Zega, T. J. and Floss, C. (2013) Extraction and analysis of a presolar oxide grain from the Adelaide ungrouped C2 chondrite. *Lunar Planet. Sci. XLIV*, #1287.

Zega, T. J., Nittler, L., Busemann, H., Hoppe, P. and Stroud, R. M. (2007) Coordinated isotopic and mineralogic analyses of planetary materials enabled by in situ lift-out with a focused ion beam scanning electron microscope. *Meteorit. Planet. Sci.* **42**, 1373–1386.

Zega, T. J., Haenecour, P., Floss, C. and Stroud, R. M. (2014) Extraction and analysis of presolar grains from the LAP 031117 CO3.0 chondrite. *Lunar Planet. Sci. XLV*, #2256.

Zhao, X., Stadermann, F. J., Floss, C., Bose, M. and Lin, Y. (2010) Characterization of presolar grains from the carbonaceous chondrite Ningqiang. *Lunar Planet. Sci. XLI*, #1431.

Zhao, X., Floss, C., Stadermann, F. J., Bose, M. and Lin, Y. (2011) Continued investigation of presolar silicate grains in the carbonaceous chondrite Ningqiang. *Lunar Planet. Sci. XLII*, #1982.

Zhao, X., Floss, C., Lin, Y. and Bose, M. (2013) Stardust investigation into the CR chondrite Grove Mountain 021710. *Astrophys. J.* **769**, doi:10.1088/0004-637X/769/1/49.

Zinner, E. (2014) Presolar grains. *Treatise on Geochemistry* (Holland, H. D. and Turekian, K. K., eds.; vol. ed. Davis, A. M.), 2nd ed., Vol. 1.4, 181–213, Elsevier Ltd., Oxford.

Zinner, E., Amari, S., Guinness, R., Nguyen, A., Stadermann, F. J., Walker, R. M. and Lewis, R. S. (2003) Presolar spinel grains from the Murray and Murchison carbonaceous chondrites. *Geochim. Cosmochim. Acta* **67**, 5083–5095.

Zinner, E., Nittler, L. R., Hoppe, P., Gallino, R., Straniero, O. and Alexander, C. M. O'D. (2005) Oxygen, magnesium and chromium isotopic ratios of presolar spinel grains. *Geochim. Cosmochim. Acta* **69**, 4149–4165.

Zinner, E., Nittler, L. R., Gallino, R., Karakas, A. I., Lugaro, M., Straniero, O. and Lattanzio, J. C. (2006) Silicon and carbon isotopic ratios in AGB stars: SiC grain data, models, and the Galactic evolution of the Si isotopes. *Astrophys. J.* **650**, 350–373.

Zinner, E. K., Moynier, F. and Stroud, R. M. (2011) Laboratory technology and cosmochemistry. *Proc. Nat.'l Acad. Sci.* **108**, 19135–19141.